

Effect of void fraction and friction factor models on the prediction of pressure drop of R134a during downward condensation in a vertical tube

Journal:	*Heat and Mass Transfer*
Manuscript ID:	HMT-10-0389
Manuscript Type:	Original Paper
Date Submitted by the Author:	10-Nov-2010
Complete List of Authors:	Dalkilic, A.; Yildiz Technical University Kuerekci, N.; Yildiz Technical Univeersity Wongwises, Somchai; King Mongkut University of Technology Thonburi, Mechanical Engineering
Keywords:	condensation heat transfer, heat transfer, friction factor, turbulent convection heat transfer

For Review

SCHOLARONE™
Manuscripts

University of Hannover, Institut of Thermodynamics, Callinstr. 36, 30167 Hannover, Germany

Effect of void fraction and friction factor models on the prediction of pressure drop of R134a during downward condensation in a vertical tube

A.S. Dalkilic[a,*], N.A. Kürekci[a], S. Wongwises[b,*]

[a]*Heat and Thermodynamics Division, Department of Mechanical Engineering, Yildiz Technical University (YTU), Yildiz, Besiktas, Istanbul 34349, Turkey*

[b]*Fluid Mechanics, Thermal Engineering and Multiphase Flow Research Lab. (FUTURE), Department of Mechanical Engineering, King Mongkut's University of Technology Thonburi (KMUTT), Bangmod, Bangkok 10140, Thailand*

Abstract

The theoretical flow models of homogeneous and separated and their modifications are applied to forced convection in-tube condensation to predict the pressure drop characteristics of R134a. Homogeneous flow model is modified by ten different average homogeneous dynamic viscosity correlations and various alternative correlations of total, frictional and momentum pressure drop to take account of the partial condensation inside the tube. In addition to this, numerical analyses were performed to determine the average and local homogeneous wall shear stresses and friction factors by means of a CFD program. Equivalent Reynolds number model is modified by six different well-know two-phase friction factors to determine the total condensation pressure drop in separated flow model. The prediction of the refrigerant side total pressure drops, frictional pressure drops, friction factors and wall shear stresses fall within ± 30% of the experimental data.

Keywords: Condensation, Pressure drop, Wall shear stress, Homogeneous flow; Separated flow, CFD

---

*Corresponding authors;

Email: dalkilic@yildiz.edu.tr; *Tel.* +902123832819; *Fax:* +902122616659

Email: somchai.won@kmutt.ac.th ; *Tel.* +6624709115; *Fax:* +6624709111

1. Introduction

Many conventional refrigerants are being phased out from industrial use since the depletion of the earth's ozone layer and global warming has been discovered. Consequently, a lot of corporations have been required to find substitute chemicals. To meet the demand for saving the environment

For Peer Review

and also improving the performance of refrigerating equipment, re-examination of the individual components is essential. The correct size of the condenser is one of the significant issues for the optimal performance of refrigerating and air conditioning systems. The design and analysis of flow and heat transfer characteristics are complex ones. The condensation of refrigerant has been investigated by numerous numbers of researchers, generally through experimental investigations. A good understanding of the two-phase flow characteristic should be included in the studies of the two-phase flow regimes, void fraction, and pressure drop. The model simulation for condensation of the refrigerant in vertical tube has received comparatively less attention in the literature.

The hydrodynamics of the condensate at the start of the tube are controlled by the shearing effect of the vapor phase if the inlet vapor flow rate is large enough. At the same time as the condensation is continuous in the tube, the vapor flow rate decreases and thus the condensate increases correspondingly. Due to occurrence of this process in the tube, a conversion caused by the effect of gravity between flow patterns appears gradually. Therefore, there is annular or mist/annular flow at the beginning of the tube and a transition to other flow patterns occur along the tube length. A big difference exists between the heat transfer behaviors of the shear and gravity controlled regimes extraordinarily, and for this reason the developed models and correlations' exactness is dependable to the correct determination of the flow patterns. The most main flow regime is the annular flow according to the studies in the literature, particularly during condensation inside tubes for high vapor qualities. It can be obtained from literature that annular flow inside tubes can exist until the vapor quality reaches a value of 0.25. As a result, the annular flow is focused by various theoretical and experimental two-phase flow investigations. By means of these investigations in the literature, the designers can solve the in-tube condensation phenomena easily.

The heat transfer characteristics of the flow in condenser tubes are affected by the heat transfer resistance of the condensate intensively. The local heat flux and the film thickness are one of the main considerable parameters. First of all, Nusselt [1] presented a well-known model that is valid for smooth films at low vapour velocities regarding the prediction of the Nusselt number and film thickness for laminar films. Wasten and Dukler [2] performed the first numerical study on the calculation of a two-dimensional wavy surface using measured film thickness during turbulent film flow. Kritsadathikarn et al. [3] modified a homogeneous two-phase flow model to investigate the flow characteristics of some refrigerants flowing in adiabatic capillary tubes. The basic governing equations are derived from the conservations of mass, energy and momentum. The Runge-Kutta method is used to solve the differential equations obtained simultaneously. According to their numerical results, the traditional refrigerants give lower pressure gradients than the alternative

For Peer Review

refrigerants used as examples in their study. Choi et al. [4] proposed a correlation from a database consisting of the following pure and mixed refrigerants: R125, R134a, R32, R410A, R22, R407C and R32/R134a (25/75 % mass). The new correlation was derived by replacing the friction factor and the tube-diameter in the Bo Pierre [5] correlation with a friction factor obtained from pressure drop data for a micro-fin tube and the hydraulic diameter, respectively. Choi et al. [6] did convective boiling pressure drop experiments using horizontal mini channels with a binary mixture refrigerant, R-410A. Their experimental results were compared against 15 two-phase pressure drop prediction methods. The experimental pressure drop was predicted by the homogeneous model successfully. A new pressure drop prediction method based on the Lockhart–Martinelli [7] method was developed with 4.02% mean deviation. In Baudouy [8]' study, pressure drop estimation was done with the momentum balance equation including subcooling. The homogeneous model and Friedel's friction multiplier [9] related with Huq and Loth [10]'s void fraction correlations determined the data within 15%. Dutkowski [11] investigated the frictional pressure drop in horizontal minichannels and compared his experimental results with the theoretical values obtained from a homogeneous equilibrium model. The dynamic viscosity correlations of McAdams et al. [12], Cicchitti et al. [13], Dukler et al. [14], Owens [15], Ackers et al. [16], Beattie and Whalley [17], and Lin et al. [18] were used in his analysis. As a result of his analysis, any of the tested correlations cannot determine the two-phase pressure drop gradient agreeably. The homogeneous model was modified with a correction factor proposed by Chen [19]. Yadigaroglu and Lahey [20] presented an alternative form for the conservation equations for one dimensional time-dependent two-phase flow. The model included the effects of the radial distributions of void fraction, velocity and enthalpy, which were taken into account through the use of spatial correlation coefficients. Later, their model was modified by Wang [21] to analyze the thermally non-equilibrium condensing flow in a double-pipe condenser. Bhramara et al. [22] did investigations at different saturation temperatures and at different flow rates to determine the local frictional pressure drop using homogeneous model. Each of the refrigerants' average properties is calculated assuming that they are considered as single phase pseudo fluid. The so obtained pressure drop data is compared with the separated flow models available in literature. Rahimi et al. [23] reported experimental and CFD investigations on the friction factor, Nusselt number and thermal-hydraulic performance of a tube equipped with the classic and three modified twisted tape inserts. According to their results, the Nusselt number and performance of the jagged insert were higher than other ones.

To the best of the authors' knowledge, no information in open literature is currently available on the combination of mathematical models of refrigerant flow and numerical solution as

For Peer Review

CFD during in-tube condensation to their application for the prediction of the pressure drop characteristics in vertical tubes. In the present study, the mathematical models of homogeneous and separated are modified to study the adiabatic steady-state one-dimensional flow of refrigerants condensing under various heat fluxes and condensing temperatures in a vertical tube. The physical properties of pure R134a belong to the homogeneous model are provided by means of various correlations. In addition to this, apart from the authors' previous publications in the literature, there are few studies in the literature using the experimental parameters of this study related with the heat transfer and pressure drop characteristics for condensation in a small diameter vertical tube during co-current down flow of R134a. As a result, the main concern of this study is to show the application of the investigated models to the annular flow condensation in a vertical tube by means of a agreeable void fraction correlation reported in the authors' previous studies, dynamic viscosity correlations, equivalent Reynolds number model [24] and some well-known two-phase friction factors from the literature using a large number of experimental pressure drops to determine the wall shear stress, friction factor, frictional ant total pressure drops. A comparison of pressure drop characteristics belonging to the model and experiment is performed, and their some results are also in agreement with the Fluent CFD program [25] in terms of the agreed correlations. The independence of pressure drop calculations from tube orientation [26] is also shown by means of the correlations valid for different tube orientations and agreed results. The local distributions of the wall shear stress and friction factor of R134a along to the tube length, calculated by Fluent CFD program [25], flowing in the test tube is also shown in this paper.

For Peer Review

2. Experimental apparatus and method

In the experimental setup, the vertical test section is a 0.5 m long countercurrent flow double tube heat exchanger with refrigerant flowing in the inner smooth copper tube (8.1 mm i.d.) and cooling water flowing in the annulus (26 mm i.d.). Detailed descriptions of the experimental apparatus for studying condensation of R134a inside a vertical tube can be found in the authors' previous publications in the literature.

3. Data reduction and experimental uncertainty

The following equations are used to prepare the system for experiments which have saturated vapor of R134a at the inlet of test section during steady-state regime conditions. Energy balances are written for evaporator and test section separately. Data reduction of measured results is summarized in the following procedures:

3.1 The inlet vapor quality of the test section ($x_{TS,i}$)

$$x_{TS,i} = \frac{i_{TS,i} - i_{l@T_{TS,i}}}{i_{fg@T_{TS,i}}} \quad (1)$$

where $i_{l@T_{TS,i}}$ is the enthalpy of the saturated liquid based on the inlet temperature of the test section, $i_{fg@T_{TS,i}}$ is the enthalpy of vaporization based on the inlet temperature of the test section, $i_{TS,i}$ is the refrigerant enthalpy at the test section inlet and is given by:

$$i_{TS,i} = i_{ph,i} + \frac{Q_{ph}}{m_{ref}} \quad (2)$$

where $i_{ph,i}$ is the inlet enthalpy of the liquid refrigerant before entering the pre-heater, m_{ref} is the mass flow rate of the refrigerant, and Q_{ph} is the heat transfer rate in the pre-heater:

$$Q_{ph} = m_{w,ph} c_{p,w} (T_{w,i} - T_{w,o})_{ph} \quad (3)$$

where $m_{w,ph}$ is the mass flow rate of the water entering the preheater, $c_{p,w}$ is the specific heat of water, $(T_{w,i} - T_{w,o})_{ph}$ is the temperature difference between inlet and outlet positions of the preheater.

3.2 The outlet vapor quality of the test section ($x_{TS,o}$)

$$x_{TS,o} = \frac{i_{TS,o} - i_{l@T_{TS,o}}}{i_{fg@T_{TS,o}}} \quad (4)$$

where $i_{TS,o}$ is the refrigerant enthalpy at the test section outlet, $i_{l@T_{TS,o}}$ is the enthalpy of the saturated liquid based on the outlet temperature of the test section, and $i_{fg@T_{TS,o}}$ is the enthalpy of vaporization. The outlet enthalpy of the refrigerant flow is calculated as follows:

$$i_{TS,o} = i_{TS,i} - \frac{Q_{TS}}{m_{ref}} \quad (5)$$

where the heat transfer rate, Q_{TS}, in the test section is obtained from:

$$Q_{TS} = m_{w,TS} c_{p,w} (T_{w,o} - T_{w,i})_{TS} \quad (6)$$

where $m_{w,TS}$ is the mass flow rate of the water entering the test section, and $(T_{w,o} - T_{w,i})_{TS}$ is temperature difference between outlet and inlet position of the test section.

For Peer Review

3.3 Modeling of the condensation in a vertical tube

The homogeneous and the separated flow models are the most important types of flow models in developing frictional pressure drop. The separated flow model assumes that there are two artificially separated streams, each flowing in its own tube. According to this model, the velocities of each phase are constant and different from each other in their cross-sections in the tube. Most of the two-phase frictional pressure drop models are related to the separated flow analysis. Moreover, it is essential to apply a properly defined single-phase friction factor to a two-phase friction factor according to the homogeneous model, which assumes an equilibrium for the flow of both phases and also equal vapor and liquid velocities (S=1). The homogeneous model is also known as the friction factor model and the frictional pressure drop is computed as if the flow were a single-phase flow according to this model.

3.3.1 Homogeneous flow model

Momentum pressure drop can be expressed either by means of Eq. (7) or Eq. (8) respectively as follows:

$$-\left(\frac{dP}{dz}\right)_M = \frac{G^2\left(x_i - x_o\right)}{L\left(\rho_l - \rho_g\right)} \tag{7}$$

$$-\left(\frac{dP}{dz}\right)_M = \frac{G^2}{L}\left(\frac{1}{\rho_o} - \frac{1}{\rho_i}\right) \tag{8}$$

Pressure drop due to gravity can be determined from Eq. (9) as:

$$-\left(\frac{dP}{dz}\right)_G = \rho_{tp} g \tag{9}$$

Experimental frictional pressure drop is calculated as follows:

$$\left(\frac{dP}{dz}\right)_F = \left(\frac{dP}{dz}\right)_{exp} - \left(\frac{dP}{dz}\right)_G - \left(\frac{dP}{dz}\right)_M \tag{10}$$

The frictional pressure drop correlations can be used to determine the two-phase friction factors in Eqs. (11) and (12) respectively as follows:

$$-\left(\frac{dP}{dz}\right)_F = \frac{2 f_{tp} G^2}{d\rho_{tp}} \tag{11}$$

For Peer Review

$$-\left(\frac{dP}{dz}\right)_F = \frac{2f_{tp}G^2}{d\rho_{tp}}\left[1+\frac{\Delta x}{2}\left(\frac{\rho_g}{\rho_l-\rho_g}\right)\right] \tag{12}$$

In addition to this, it is possible to calculate the frictional pressure drop by means of the approach of two-phase multiplier as follows:

$$-\left(\frac{dP}{dz}\right)_F = \frac{2f_{tp}G^2}{d\rho_l}\phi_l{}^2 \tag{13}$$

where the two-phase friction factor is determined as follows:

$$\phi_l{}^2 = \left(1+x\left(\frac{\nu_g-\nu_l}{\nu_l}\right)\right)\left(1+x\left(\frac{\mu_l-\mu_g}{\mu_g}\right)\right)^{-0.25} \tag{14}$$

Wall shear stress is calculated as follows:

$$\tau_{wall} = \frac{f_{tp}\rho_{tp}u_{hom}{}^2}{2} \tag{15}$$

where the homogeneous velocity is calculated from Dutkowski's [11] study as:

$$u_{hom} = \frac{m_{total}}{\rho_{tp}A} \tag{16}$$

where the total mass flow is calculated as:

$$m_{total} = GA \tag{17}$$

and the area of the flow can be calculated as:

$$A = \frac{\pi d^2}{4} \tag{18}$$

The homogeneous dynamic viscosity correlations (μ_{tp}) in the literature are summarized in Table 1. They were the variable parameters in the related equations in the study and also numerical solution of the study.

Table 1 Homogeneous dynamic viscosity correlations

The Fanning friction factor can be calculated using the Hagen-Poiseuille flow [31] in Eq. (19) for laminar-laminar flow and the Blasius equation [32] in Eq. (20) for turbulent-turbulent flow respectively as follows:

$$Re_{hom}<2300 \qquad f_{tp} = \frac{16}{Re_{hom}} \tag{19}$$

For Peer Review

$$Re_{hom}>2300 \qquad f_{tp} = \frac{0.079}{Re_{hom}^{0.25}} \tag{20}$$

where the homogeneous Reynolds number can be determined as:

$$Re_{hom} = \frac{Gd}{\mu_{tp}} \tag{21}$$

3.3.2 Separated flow model

The two-phase pressure gradient is the sum of three contributions: the gravitational pressure gradient, the momentum pressure gradient and the frictional pressure gradient as follows:

$$\frac{dP}{dz} = \left(\frac{dP}{dz}\right)_G + \left(\frac{dP}{dz}\right)_M + \left(\frac{dP}{dz}\right)_F \tag{22}$$

Pressure drop due to gravity can be determined as [33]:

$$(\Delta P)_G = g(\alpha\rho_g + (1-\alpha)\rho_l)L \tag{23}$$

where the void fraction, α, can be determined from Chisholm [34] correlation shown in Table 2.

Table 2 Void fraction models and correlations

Generally, the characterization of two-phase flows depends on the void fraction which is a major value for the calculation of various parameters regarding with the heat transfer and pressure drop. Accordingly, researchers have performed intensive studies to develop void fraction correlations for two-phase flows. In consequence of their efforts in the literature, Void fraction models and correlations can be specified as local, chordal, cross-sectional, and volumetric for different flow regimes. It should be noted that determination of the proper void fraction models and correlations belong to the authors' experimental database were performed in the authors' previous publications and agreed void fraction models and correlations are summarized in Table 2.

The momentum transfer term contributes to the overall pressure drop during condensation due to the mass transfer that occurs at the phase's interface. It was reported in the literature that the momentum pressure gradient can be neglected for the condensation, on the other hand, the momentum pressure gradient can be written according to the results of the one-dimensional two-phase separated-flow analysis which can be defined as follows:

$$\left(\frac{dP}{dz}\right)_M = -G^2 \frac{d}{dz}\left[\frac{x^2}{\rho_g \alpha} + \frac{(1-x)^2}{\rho_l(1-\alpha)}\right] \tag{24}$$

For Peer Review

Eq. (24) can be rearranged as follows:

$$\Delta P_M = G^2\left[\left\{\frac{(1-x)^2}{\rho_l(1-\alpha)}+\frac{x^2}{\rho_g\alpha}\right\}_o-\left\{\frac{(1-x)^2}{\rho_l(1-\alpha)}+\frac{x^2}{\rho_g\alpha}\right\}_i\right] \quad (25)$$

Akers et al. [39] developed a two-phase multiplier with the assumption that two-phase flows were similar to a single-phase flow. He predicted the frictional two-phase pressure drop by means of a multiplying factor, using the same rationale as that behind the Lockhart Martinelli multiplier [7]. His model is known as the "equivalent Reynolds number model". It can be used for an annular flow regime which could be replaced by an equivalent all liquid flow that produces the same wall shear stress as that of the two-phase flow according to this model. The two-phase frictional pressure drop is calculated from two-phase friction factor by the following equation based on all liquid Re number [39] as follows:

$$f_{tp} = \frac{(\Delta P)_F}{G_{eq}^{\ 2}/2\rho_l}\frac{d}{4L} = \frac{(\Delta P)_F 2\rho_l d^3}{Re_{eq}^{\ 2}\mu_l^{\ 2}4L} \quad (26)$$

where the all liquid equivalent Re number is determined from:

$$Re_{eq} = \frac{G_{eq}d}{\mu_l} \quad (27)$$

and equivalent liquid mass flux is defined as:

$$G_{eq} = G\left((1-x)+x\left(\frac{\rho_l}{\rho_g}\right)^{0,5}\right) \quad (28)$$

and two-phase friction factors are calculated by means of the correlations in Table 3.

Table 3 Friction factor models and correlations

Fukano and Furukawa [40] investigated the effects of liquid viscosity on the mean liquid film thickness, wave heights, and gas-liquid interfacial stresses in the vertical upward co-current annular flow in a 26 mm inner diameter tube using water and glycerol solutions as working fluids. Moeck [41] performed experiments on the diameter of entrained liquid droplets for air-water annular flow. Fore et al. [42] has obtained the film thickness and pressure gradient data for co-current upward flow of nitrogen and water under high pressure in a rectangular duct. Carey [43] developed Blasius's [32] friction factor and reported that the vapour flow in the tube can be treated as a single phase flow. Because the film is thin, the mean velocity of vapour is much larger than the

For Peer Review

liquid velocity at the interface due to the high viscosity of the liquid phase compared to the vapour phase. Moreover, vapour velocity is assumed to be zero between the phases. The interfacial shear can be computed using the conventional single phase correlation by using these assumptions. Interfacial shear stress in annular two-phase flow is one of the main parameters governing transport phenomena and is required for modeling the flow. It has been intensively studied, especially for the flow assuming that all liquid travels in the liquid film.

3.3.3 Numerical model

This problem was solved by means of the processes in Fluent CFD program [25]. Fluent is commonly used software in CFD analysis in the literature and a detailed description of the mathematical model can be found in the Fluent User's Guide. This program uses a technique based on control volume theory to convert the governing equations to algebraic equations so they can be solved numerically. The control volume technique works by performing the integration of the governing equations about each control volume, and then generates discrimination of the equations which conserve each quantity based on control volume. Details of the selections in CFD program is given in Table 4. The necessary input values for the CFD program to run are obtained from the homogeneous flow model's correlations such as dynamic viscosity from Lin et al. [18].

The skin friction coefficient is defined by,

$$C_f = \frac{\tau_{wall}}{\frac{1}{2}\rho U_\infty^{\,2}} \tag{29}$$

where τ_{wall} is the local wall shear stress, ρ is the fluid density and U_∞ is the free-stream velocity (usually taken ouside of the boundary layer or at the inlet).

The wall shear stress, τ_{wall}, is given by,

$$\tau_{wall} = \mu\left(\frac{\partial u}{\partial y}\right)_{y=0} \tag{30}$$

where μ is the dynamic viscosity, u is the flow velocity parallell to the wall and y is the distance to the wall.

4. Results and discussion

The indirectly determined void fraction, wall shear stress, friction factor, frictional pressure drop and total pressure drop were presented in the following paragraphs using a large number of

For Peer Review

measured data during the downward laminar condensation of R134a at a high mass flux in a vertical smooth tube over a range of experimental conditions shown in authors' previous publications. It should be noted that detailed explanations and some additional figures and tables with different experimental parameters related to this study on the void fraction models and correlations, film thickness models, friction factor and frictional pressure drop models, and heat transfer and pressure drop characteristics of data belonging to the experimental apparatuses can be seen in the authors' previous publications in the literature.

The experiments were performed at the Fluid Mechanics, Thermal Engineering and Multiphase Flow Research Laboratory (FUTURE) in KMUTT in order to investigate the effect of empirical correlations such as dynamic viscosity correlations and friction factor correlations on the pressure drop characteristics using well-known flow models for the downward two-phase flow of R134a in a vertical round tube with an inner diameter of 8.1 mm. Pure HFC-134a was used in the experiments. The heat fluxes are between 10.16 and 66.61 kW/m^2 while the mass fluxes are between 260 and 515 kg/m^{2}s. The discussion of the results is presented as follows:

The data shown in all tables and figures for the study of R134a condensation in a vertical tube were found in the annular flow section according to the authors' investigation of flow identification studies using various flow pattern maps and correlations and also checked by sight glass at the inlet and outlet of the test section.

The pressure drop is obtained by dividing the measured pressure drop by the length between pressure taps. In the vertical test section, the length between pressure taps is 0.7 m while the length of the heat exchanger is 0.5 m.

Table 2 shows the void fraction models and correlations that agree with the experimental database according to the authors' investigation of void fraction studies. As a result of the analysis, these void faction models and correlations give quite similar values such as gravitational and momentum pressure drops. For that reason, the Chisholm correlation [34] is used as a constant void faction correlation in the analysis.

Plots of the results belong to the homogeneous flow model are given from Figs. 1 to 12. The variations in these figures to calculate the two-phase friction factor, wall shear stress, frictional pressure drop and total pressure drop are generated by means of the two-phase homogeneous dynamic viscosity correlations such as Mc Adams et al. [12], Cicchitti et al. [13], Dukler et al. [14], Ovens [15], Ackers [16], Beattie and Whalley [17], Lin et al. [18], Fourar and Bories [28], Davidson [29], Garcia et al. [30]. Alternative correlations from the literature are gathered for the determination of momentum pressure drop in Eqs. (7) and (8), and frictional pressure drop in Eqs.

For Peer Review

(11) and (12). The effects of these equations on the determined values are investigated in the paper. It should be noted that the two-phase homogeneous dynamic viscosity correlations of Fourar and Bories [28], and Davidson [29] have considerably large deviations from the experimental data due to their incompatible operating conditions; therefore, they are not presented in most of the figures.

Figs. 1 and 2 show the comparison of two-phase friction factors calculated based on Blasius [32] equation according to the dynamic viscosity correlations in Table 1 and different frictional pressure drop correlations in Eqs. (11) and (12). As a result of these plots, the two-phase friction factor obtained from Eq. (11) is found to be more predictive than those obtained by Eq. (12) according to Mc Adams et al. [12], Dukler et al. [14], Ovens [15], Lin et al. [18] and Garcia et al. [30]'s two-phase homogeneous dynamic viscosity correlations.

For the same purpose in Figs. 1 and 2, the two-phase homogeneous friction factors are determined by means of CFD program [25] in Fig. 3 according to Lin et al.'s [18] dynamic viscosity correlation. Numerical results are found to be in good agreement with those obtained from Eq. (11) as the same with the theoretical results. Fig. 4 shows local variation of the two-phase homogeneous friction factors obtained from the numerical study. Their local values increase gradually along the tube length as expected.

Fig. 1 Comparison of two-phase friction factors obtained from Blasius [32] equation and Eq. (11)

Fig. 2 Comparison of two-phase friction factors obtained from Blasius [32] equation and Eq. (12)

Fig. 3 Comparison of two-phase friction factors obtained from Eq. (11) (a) and (b) Eq. (12) and CFD program [25]

Fig. 4 Local alterations of two-phase friction factors obtained from CFD program [25] for various experimental conditions

In a similar way with the last figures, Figs. 5 and 6 show the comparison between the calculated wall shear stresses obtained from Eq. (13) and experimental ones. Fig. 7 shows the numerical results for the determination of wall shear stress. Consequently, similar results with the previous one, where the majority of the data belong to agreed correlations fall within the ± 30% deviation band, obtained from these figures. Fig. 8 illustrates the local wall shear stress values

For Peer Review

obtained from CFD program [25]. Characteristics of the trend lines in the figure are in good agreement with those in the literature.

Fig. 5 Comparison of wall shear stresses obtained from Eq. (13) and Eq. (11)

Fig. 6 Comparison of wall shear stresses obtained from Eq. (13) and Eq. (12)

Fig. 7 Comparison of wall shear stresses obtained from Eq. (11) (a) and (b) Eq. (12) and CFD program [25]

Fig. 8 Local alterations of wall shear stresses obtained from CFD program [25] for various experimental conditions

It can be clearly seen from Figs. 9 and 10 that the agreed results come from the two-phase homogeneous dynamic viscosity of Mc Adams et al. [12], Dukler et al. [14], Ovens [15], Lin et al. [18] and Garcia et al. [30] as expained before. The effect of the usage of the different momentum pressure drop correlations in Eqs. (7) and (8) are also shown in these figures. Similar prediction performance is seen for the momentum pressure drop equations. The frictional pressure drop correlation in Eq. (11) is used in this figures.

Fig. 9 Comparison of frictional pressure drops obtained from Eqs. (7), (10) and Eq. (11)

Fig. 10 Comparison of frictional pressure drops obtained from Eqs. (8), (10) and Eq. (11)

Another frictional pressure drop correlation in Eq. (13) is used for the calculations in Figs. 11 and 12. Ssme variables with the previous figure are also used in these figures to investigate their effects. Altough the dynamic viscosity correlations of Cicchitti et al. [13], Ackers [16], and Beattie and Whalley [17] have better prediction performance than others, none of them has satisfactory results for all experimental conditions in these figures.

Fig. 11 Comparison of frictional pressure drops obtained from Eqs. (7), (10) and Eq. (13)

Fig. 12 Comparison of frictional pressure drops obtained from Eqs. (8), (10) and Eq. (13)

For Peer Review

Plots of the results belong to the separated flow model are given from Figs. 13 to 16. The variations in these figures to calculate the two-phase total pressure drop are generated by means of the two-phase friction factor correlations such as Fukano and Furukawa [40], Moeck [41], Fore et al. [42], Choi et al. [6], and Carey [43]. Elimination process are performed in Fig. 13 to determine the best predictive friction factors. As a result, the friction factors of Moeck [41], Fore et al. [42] and Choi et al. [6] are found to be better than others. It can be clearly seen from Figs. 14 and 15 that the distribution of the data between the error bands of ± 30% seems quite balanced. It should be noted that the data in these figures belong to the laminar flow and none of these friction factors apart from Choi et al. [6] in Fig. 16 could not predict the total pressure drop during turbulent flow due to their large deviations from the experimental values. The prediction success of Choi et al. [6]'s correlation can be seen from Fig. 16 for laminar and turbulent flow data within the deviation of ± 30%. Total pressure drop increases with increasing mass fluxes in all figures as expected.

Fig. 13 Comparison of total pressure drop values between measured and calculated ones obtained from Eq. (22) during laminar flow of R134a

Fig. 14 Comparison of total pressure drop values between measured and calculated ones obtained from Eq. (22) and Moeck [41]'s two-phase friction factor during laminar flow of R134a

Fig. 15 Comparison of total pressure drop values between measured and calculated ones obtained from Eq. (22) and Fore et al. [42]'s two-phase friction factor during laminar flow of R134a

Fig. 16 Comparison of total pressure drop values between measured and calculated ones obtained from Eq. (22) and Choi et al. [6]'s two-phase friction factor during laminar and turbulent flows of R134a

5. Conclusion

Experiments have been performed to predict the pressure drop characteristics using homogeneous and separated flow models by means of the proper two-phase dynamic viscosity correlations, some alternative correlations of momentum and pressure drop and various two-phase friction factors and void fraction models and correlations. There is little research on the parameters and content used in this study in the current literature. The content of this study is expected to fill this gap in the

For Peer Review

literature. Accurate experiments were done for annular flow heat transfer data in a vertical tube for the condensation of R134a at high mass flux. The importance of the usage of a large number of data with different experimental conditions is shown during validation process of the results.

The calculated homogeneous two-phase friction factors, wall shear stresses, frictional pressure drops and total pressure drops by means of Mc Adams et al., Dukler et al., Ovens, Lin et al. and Garcia et al.'s two-phase homogeneous dynamic viscosity correlations are found to be in good agreement with the experimental data within the ± 30% deviation band.

Moreover, correlations of the two-phase friction factors of Moeck and Fore et al. for the laminar flow and Choi et al. for the laminar and turbulent flows are the best predictive models within the ± 30% deviation band for the investigation of the separated flow model's total pressure drop correlation and could reflect the effect of mass flux on the total pressure drop.

Acknowledgments

The authors would like to thank King Mongkut's University of Technology Thonburi (KMUTT), the Thailand Research Fund, the Office of Higher Education Commission and the National Research University Project for the financial support. Especially, the first author wishes to thank KMUTT for providing him with a Post-doctoral fellowship.

Nomenclature

A	inside surface area, m^2
CFD	computational fluid dynamics
C_f	non-dimensional skin friction coefficient
c_p	specific heat, J/kgK
d	internal tube diameter, m
f	friction factor
G	mass flux, kg/m^2s
g	gravitational constant m/s^2
i	enthalpy, J/kg
i_{fg}	latent heat of condensation, J/kg
L	length of test tube, m
m	mass flow rate, kg/s
P	pressure, MPa
Re	Reynolds number

For Peer Review

S	slip ratio
T	temperature, °C
u	velocity, m/s
U_∞	free stream velocity, m/s
Q	heat transfer rate, W
q	mean heat flux, kW/m
x	mean vapor quality
y	wall coodinate
z	wall coordinate
ΔP	pressure drop, Pa
ΔT	vapor side temperature difference, T_{sat}-T_{wi}, K

Greek Symbols

$\square_l^2$	two-phase multiplier
ρ	density, kg m^{-3}
μ	dynamic viscosity, kg/ms
α	void fraction
δ	film thickness, m
τ	shear stress, N/m
ν	specific volume, m^3/kg

Subscripts

eq	equivalent
exp	measured
F	frictional term
G	gravitational term
g	gas/vapor
hom	homogeneous
i	inlet
l	liquid
loc	local
o	outlet

For Peer Review

ph	preheater
ref	refrigerant
sat	saturation
TS	test section
tp	two-phase
w	water

References

[1] W. Nusselt, Die Oberflachen Kondenastion des Wasserdamfes, Zeitschrift des Vereines Deutscher Ingenieure 60(1916) 541–546, 569–575.

[2] F.K. Wasden and A.E. Dukler, Insights into the hydrodynamics of free falling wavy films, A.I.Ch.E. Journal 35 (1989) 187-195.

[3] P. Kritsadathikarn, T. Songnetichaovalit, N. Lokathada, S.Wongwises, Pressure distribution of refrigerant flow in an adiabatic capillary tube, Science Asia 28 (2002) 71-76.

[4] J.Y. Choi, M.A. Kedzierski, P.A. Domanski, A generalized pressure drop correlation for evaporation and condensation of alternative refrigerants in smooth and micro-fin tubes, NISTIR 6333 (1999) 1-50.

[5] B. Pierre, Flow resistance with boiling refrigerants-part 1, ASHRAE Journal 6 (1964) 58-65.

[6] K. Choi, A.S. Pamitran, C.Y. Oh, J.T. Oh, Two-phase pressure drop of R-410A in horizontal smooth minichannels, International Journal of Refrigeration 31 (2008) 119-129.

[7] R.W. Lockhart, R.C. Martnelli, Proposed correlation of data for isothermal two-phase, two-component flow in pipes, Chemical Engineering Progress 45 (1949) 39-48.

[8] B. Baudouy, Pressure drop in two-phase He I natural circulation loop at low vapor quality, P.S.G. Gistau Baguer (Ed.), International Cryogenic Engineering Proceedings 19 (2002) 817-820, France.

[9] L. Friedel, Improved friction pressure drop correlations for horizontal and vertical two phase pipe flow, European Two-phase Flow Group Meeting 18 (1979) 485-491.

[10] R.H. Huq, J.L. Loth, Analytical two-phase flow void prediction method, Journal of Thermophysics 6 (1992) 139-144.

[11] K. Dutkowski, Air-water two-phase frictional pressure drop in minichannels, Heat Transfer Engineering 31(2010) 321-330.

[12] W.H. McAdams, W.K. Woods, L.C. Heroman, Vaporization inside horizontal tubes II-benzene-oil mixtures, Transactions of ASME 64 (1942) 193-200.

For Peer Review

[13] A. Cicchitti, C. Lombaradi, M. Silversti, G. Soldaini, R. Zavattarlli, Two-phase cooling experiments- pressure drop heat transfer burnout measurements, Energia Nucleare 7 (1960) 407-425.

[14] A.E. Dukler, Wicks Moye, R.G. Cleveland, Frictional pressure drop in two-phase flow. Part A: a comparison of existing correlations for pressure loss and holdup, and Part B: an approach through similarity analysis, AIChE Journal 10 (1964) 38-51.

[15] W.L. Owens, Two-phase pressure gradient, ASME Int. Develop. Heat Transf. Part II (1961) 63-368.

[16] J. Lee, I. Mudawar, Two-phase flow in high-heat-flux micro-channel heat sink for refrigeration cooling applications: part II-heat transfer characteristics, International Journal of Heat and Mass Transfer 48 (2005) 941-955.

[17] D.R.H. Beattie, P.B. Whalley, Simple two-phase frictional pressure drop calculation method, International Journal of Multiphase Flow 8 (1982) 83-87.

[18] S. Lin, C.C.K. Kwok, R.Y. Li, Z.H. Chen, Z.Y. Chen, Local frictional pressure drop during vaporization for R-12 through capillary tubes, International Journal of Multiphase Flow 17 (1991) 95-102.

[19] I.Y. Chen, K.S. Yang, Y.J. Chang, C.C. Wang, Two- phase pressure drop of air-water and R-410A in small horizontal tubes, International Journal of Multiphase Flow 27 (2001) 1293-1299.

[20] H. Yadigaroglu, R.T. Lahey Jr., On the various forms of the conservation equations in two-phase flowInternational Journal of Multiphase Flow 2 (1976) 477-494.

[21] C.C. Wang, A numerical method for thermally non-equilibrium condensing flow in a double-pipe condenser, Applied Thermal Engineering 17 (1997) 647-660.

[22] P. Bhramara, V. D. Rao, K. V. Sharma , T. K. K. Reddy, CFD analysis of two phase flow in a horizontal pipe-prediction of pressure drop, International Journal of Mechanical, Industrial and Aerospace Engineering 3 (2009) 81-87.

[23] M. Rahimi, S. R. Shabaniana, A. A. Alsairafi, Experimental and CFD studies on heat transfer and friction factor characteristics of a tube equipped with modified twisted tape inserts, Chemical Engineering and Processing 48 (2009) 762-770.

[24] K. Moser, R.L. Webb, B. Na, A new equivalent Reynolds number model for condensation in smooth tubes, International Journal of Heat Transfer (1998) 410-417.

[25] Fluent release 6.2.16, Fluent Incorporated, (2005).

[26] S.L. Chen, F.M. Gerner, C.L. Tien, General film condensation correlations, Experimental Heat Transfer 1 (1987) 93-107.

For Peer Review

[27] S.J. Kline, F.A. McClintock, Describing uncertainties in single sample experiments, Mechanical Engineering 75 (1953) 3-8.

[28] M. Fourar, S. Bories, Experimental study of air–water two-phase flow through a fracture (narrow channel), International Journal of Multiphase Flow 21 (1995) 621-637.

[29] W.F. Davidson, P.H. Hardie, C.G.R. Humphreys, A.A. Markson, A.R. Mumford, T. Ravese, Studies of heat transmission through boiler tubing at pressures from 500-3300 Lbs, Transactions of ASME 65 (1943) 553-591.

[30] F. García, R. García, J.C. Padrino, C. Mata, J.L. Trallero, D.D. Joseph, Power law composite power law friction factor correlations for laminar turbulent gas- liquid flow in horizontal pipelines, International Journal of Multiphase Flow 29 (2003) 1605-1624.

[31] F.M. White, Viscous Fluid Flow, McGraw-Hill Book Co., 2005.

[32] H. Blasius, Das Ähnlichkeitsgesetz bei Reibungsvorgängen in Flüssikeiten, Forsch. Gebiete Ingenieurw 131 (1913).

[33] V.P. Carey, Liquid-Vapor Phase Change Phenomena, Hemisphere Publishing, 1992.

[34] D. Chisholm, Two phase flow in pipelines and heat exchangers, George Godwin in association with The Institution of Chemical Engineers, London, 1983.

[35] H.M. Soliman, On the annular-to-wavy flow pattern transition during condensation inside horizontal tubes, The Canadian Journal of Chemical Engineering 60 (1982) 475-481.

[36] S.L. Smith, Void fractions in two-phase flow: a correlation based upon an equal velocity head model, Proceedings of the Institution of Mechanical Engineers 36 (1969) 647-664.

[37] J.M. Turner, G.B.Wallis, The separate-cylinders model of two-phase flow, paper no. NYO-3114-6, Thayer's School Eng.,Dartmouth College, Hanover, NH, USA, 1965.

[38] P.L. Spedding, D.R. Spence, Prediction of holdup in two phase flow, International Journal of Engineering Fluid Mechanics 2 (1989) 109-118.

[39] W.W. Akers., A. Deans, O.K. Crosser, Condensing heat transfer within horizontal tubes, Chemical Engineering Progress Symposium Series 55 (1959) 171-176.

[40] T. Fukano, T. Furukawa, Prediction of the effects of liquid viscosity on interfacial shear and frictional pressure drop in vertical upward gas-liquid annular flow, International Journal of Multiphase Flow 24 (1998) 587-603.

[41] E.O. Moeck, Annular-dispersed two-phase flow and critical heat flux, AECL-3656 (1970) 337.

[42] L.B. Fore, S.G. Beus, R.C. Bauer, Interfacial friction in gas-liquid annular flow: analogies to full and transition roughness, International Journal of Multiphase Flow 26 (2000) 1755-1769.

For Peer Review

Table 1 Homogeneous dynamic viscosity correlations

Number	Homogeneous dynamic viscosity correlation	Correlation
1	Mc Adams et al. [12]	$\frac{1}{\mu_{tp}} = \frac{x}{\mu_g} + \frac{(1-x)}{\mu_l}$
2	Cicchitti et al. [13]	$\mu_{tp} = x\mu_g + (1-x)\mu_l$
3	Dukler et al. [14]	$\mu_{tp} = \rho_{tp}\left[x\nu_g\mu_g + (1-x)\nu_l\mu_l\right] = \rho_{tp}\left[x\frac{\mu_g}{\rho_g} + (1-x)\frac{\mu_l}{\rho_l}\right]$
4	Ovens [15]	$\mu_{tp} = \mu_l$
5	Ackers [16]	$\mu_{tp} = \frac{\mu_l}{(1-x) + x\left(\frac{\rho_l}{\rho_g}\right)^{0.5}}$
6	Beattie and Whalley [17]	$\mu_{tp} = \alpha_H\mu_g + \mu_l(1-\alpha_H)(1+2.5\alpha_H)$ $\alpha_H = \frac{x\rho_l}{x\rho_l + (1+x)\rho_g}$ $\mu_{tp} = \mu_l - 2.5\mu_l\left(\frac{x\rho_l}{x\rho_l + (1-x)\rho_g}\right)^2 + \left(\frac{x\rho_l(1.5\mu_l + \mu_g)}{x\rho l + (1-x)\rho_g}\right)$
7	Lin et al. [18]	$\mu_{tp} = \frac{\mu_l\mu_g}{\mu_g + x^{1.4}(\mu_l - \mu_g)}$
8	Fourar and Bories [28]	$\mu_{tp} = \rho_H\left(x\eta_g + (1-x)\eta_l + 2\sqrt{x(1-x)\eta_g\eta_l}\right) = \rho_H\left(\sqrt{x\eta_g} + \sqrt{(1-x)\eta_l}\right)$ $\eta_{tp} = \left(\sqrt{x\eta_g} + \sqrt{(1-x)\eta_g\eta_l}\right)^2$
9	Davidson [29]	$\mu_{tp} = \mu_l\left[1 + x\left(\frac{\rho_l}{\rho_g} - 1\right)\right]$
10	Garcia et al. [30]	$\mu_{tp} = \mu_l\left(\frac{\rho_H}{\rho_l}\right) = \frac{\mu_l\rho_g}{x\rho_l + (1-x)\rho_g}$

For Peer Review

Table 2 Void fraction models and correlations

Number	Void Fraction Model/Correlation	Model/Correlation
1	Homogeneous model	$\alpha_H = \dfrac{1}{1+\left(\dfrac{1-x}{x}\right)\left(\dfrac{\rho_g}{\rho_l}\right)S}$ $S = 1$
2	Chisholm [34]	$\alpha = \dfrac{1}{\alpha_H + (1-\alpha_H)^{0.5}}\alpha_{hom}$ $\alpha = 1 - \dfrac{4\delta}{d}$
3	Soliman [35]	$G(1-x) = 4\rho_l u_l\left(\dfrac{\delta}{d}\right)$
4	Smith [36]	$\alpha = \left\{1+\left(\dfrac{\rho_g}{\rho_l}\right)K\left(\dfrac{1}{x}-1\right)+\left(\dfrac{\rho_g}{\rho_l}\right)(1-K)\left(\dfrac{1}{x}-1\right)\left[\dfrac{\left(\dfrac{\rho_l}{\rho_g}\right)+K\left(\dfrac{1}{x}-1\right)}{1+K\left(\dfrac{1}{x}-1\right)}\right]\right\}^{-1}$ $K = 0.4$
5	Turner and Wallis [37]	$\dfrac{1-\alpha}{\alpha} = A\left(\dfrac{1-x}{x}\right)^p\left(\dfrac{\rho_g}{\rho_l}\right)^q\left(\dfrac{\mu_l}{\mu_g}\right)^r$
6	Spedding and Spence [38]	$\alpha = \left(1+2.22\left(\dfrac{1-x}{x}\right)^{0.65}\left(\dfrac{\rho_g}{\rho_l}\right)^{0.65}\right)^{-1}$

Correlation or model	A	p	q	r
Homogeneous	1	1	1	0
Zivi	1	1	0.67	0
Turner-Wallis	1	0.72	0.4	0.08
Lockhart-Martinelli	0.28	0.64	0.36	0.07
Thom	1	1	0.89	0.18
Baroczy	1	0.74	0.65	0.13

For Peer Review

Table 3 Friction factor models and correlations

Number	Void Fraction Model/Correlation	Model/Correlation
1	Fukano and Furukawa [40]	$f_i = 0.425\left[12+\left(\frac{\nu_l}{\nu_w}\right)\right]^{-1.33}\left(1+12\left(\frac{\delta}{d}\right)\right)$
2	Moeck [41]	$f_i = 0.005\left[1+1458\left(\frac{\delta}{d}\right)^{1.42}\right]$
3	Fore et al. [42]	$f_i = 0.005\left[1+300\left(\frac{\delta}{d}-0.0015\right)\right]$
4	Choi et al. [6]	$f = 0.00506\,Re_{fo}^{-0.0951}\,K_f^{0.1554} \quad Re=\frac{Gd}{\mu_l} \quad K_f=\frac{\Delta xi_{fg}}{Lg}$
5	Carey [33]	$f_g = 0.079\left[\frac{Gx(d-\delta)}{\mu_g(1-4\delta/d)}\right]^{-0.25}$

For Peer Review

Table 4 Details of the modelling in Fluent CFD program [25]

Viscos Model	K-epsilon standart model	
Pressure-Velocity Coupling	SIMPLE model	
Pressure	PRESTO	
Momentum	Second order upwind model	
Turbulent Kinetic Energy	Second order upwind model	
Turbulent Dissipation Rate	Second order upwind model	
Energy	Second order upwind model	
Some important critic values (iteration number: 2500)		
Residual	**Fluent Absolute Criteria**	**Criteria in the Solution**
Continuity	10^{-3}	10^{-8}
x-velocity	10^{-3}	10^{-12}
y-velocity	10^{-3}	10^{-12}
energy	10^{-3}	10^{-12}
k	10^{-3}	10^{-12}
epsilon	10^{-3}	10^{-12}

For Peer Review

FIGURE CAPTIONS

Fig. 1 Comparison of two-phase friction factors obtained from Blasius [32] equation and Eq. (11)

Fig. 2 Comparison of two-phase friction factors obtained from Blasius [32] equation and Eq. (12)

Fig. 3 Comparison of two-phase friction factors obtained from Eq. (11) (a) and (b) Eq. (12) and CFD program [25]

Fig. 4 Local alterations of two-phase friction factors obtained from CFD program [25] for various experimental conditions

Fig. 5 Comparison of wall shear stresses obtained from Eq. (13) and Eq. (11)

Fig. 6 Comparison of wall shear stresses obtained from Eq. (13) and Eq. (12)

Fig. 7 Comparison of wall shear stresses obtained from Eq. (11) (a) and (b) Eq. (12) and CFD program [25]

Fig. 8 Local alterations of wall shear stresses obtained from CFD program [25] for various experimental conditions

Fig. 9 Comparison of frictional pressure drops obtained from Eqs. (7), (10) and Eq. (11)

Fig. 10 Comparison of frictional pressure drops obtained from Eqs. (8), (10) and Eq. (11)

Fig. 11 Comparison of frictional pressure drops obtained from Eqs. (7), (10) and Eq. (13)

Fig. 12 Comparison of frictional pressure drops obtained from Eqs. (8), (10) and Eq. (13)

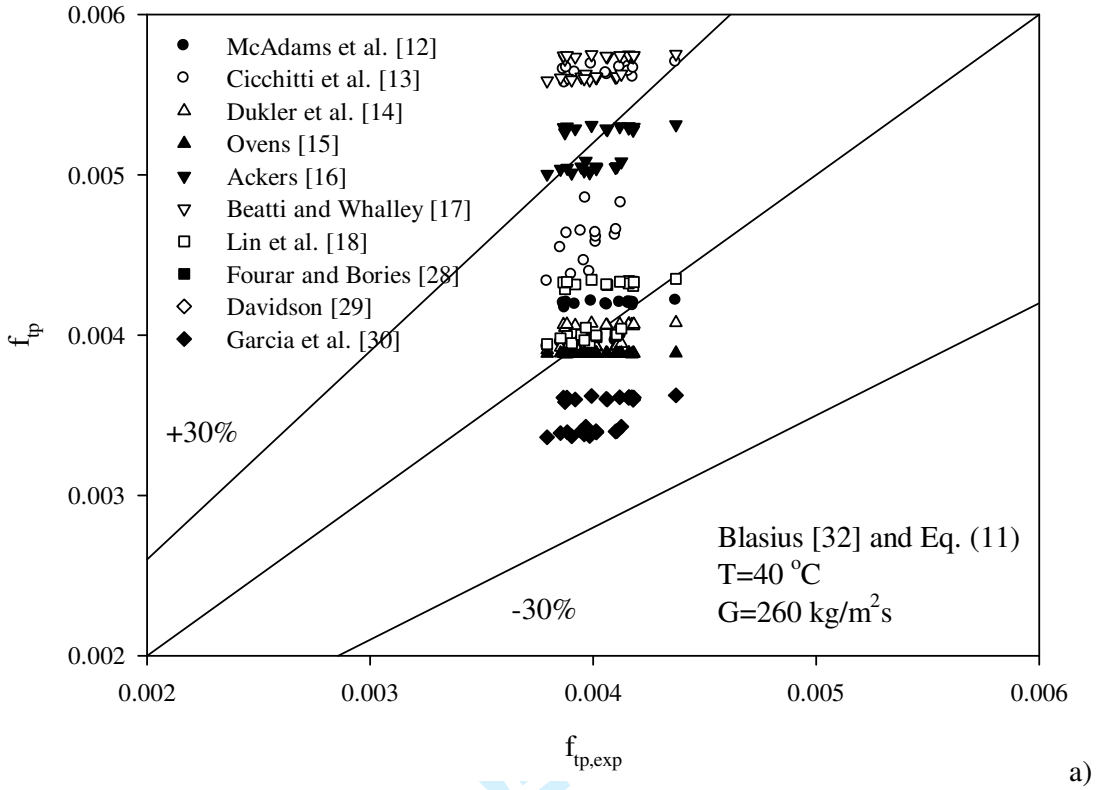
Fig. 13 Comparison of total pressure drop values between measured and calculated ones obtained from Eq. (22) during laminar flow of R134a

Fig. 14 Comparison of total pressure drop values between measured and calculated ones obtained from Eq. (22) and Moeck [41]'s two-phase friction factor during laminar flow of R134a

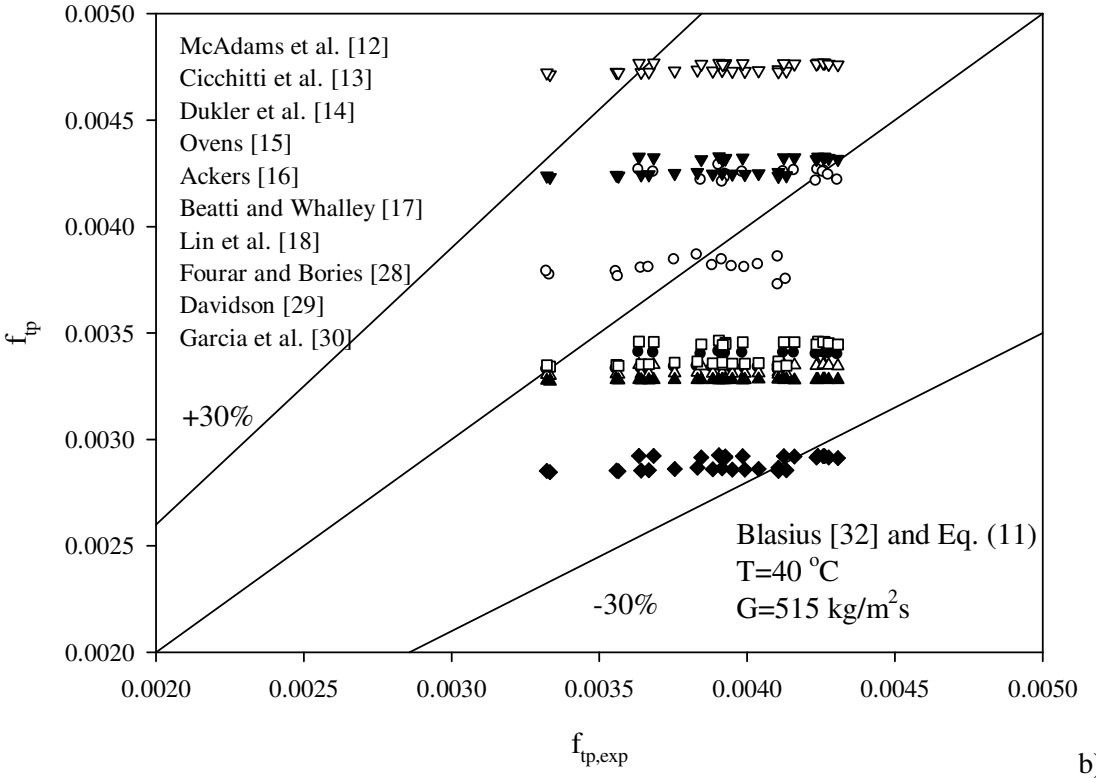
Fig. 15 Comparison of total pressure drop values between measured and calculated ones obtained from Eq. (22) and Fore et al. [42]'s two-phase friction factor during laminar flow of R134a

Fig. 16 Comparison of total pressure drop values between measured and calculated ones obtained from Eq. (22) and Choi et al. [6]'s two-phase friction factor during laminar and turbulent flows of R134a

For Peer Review

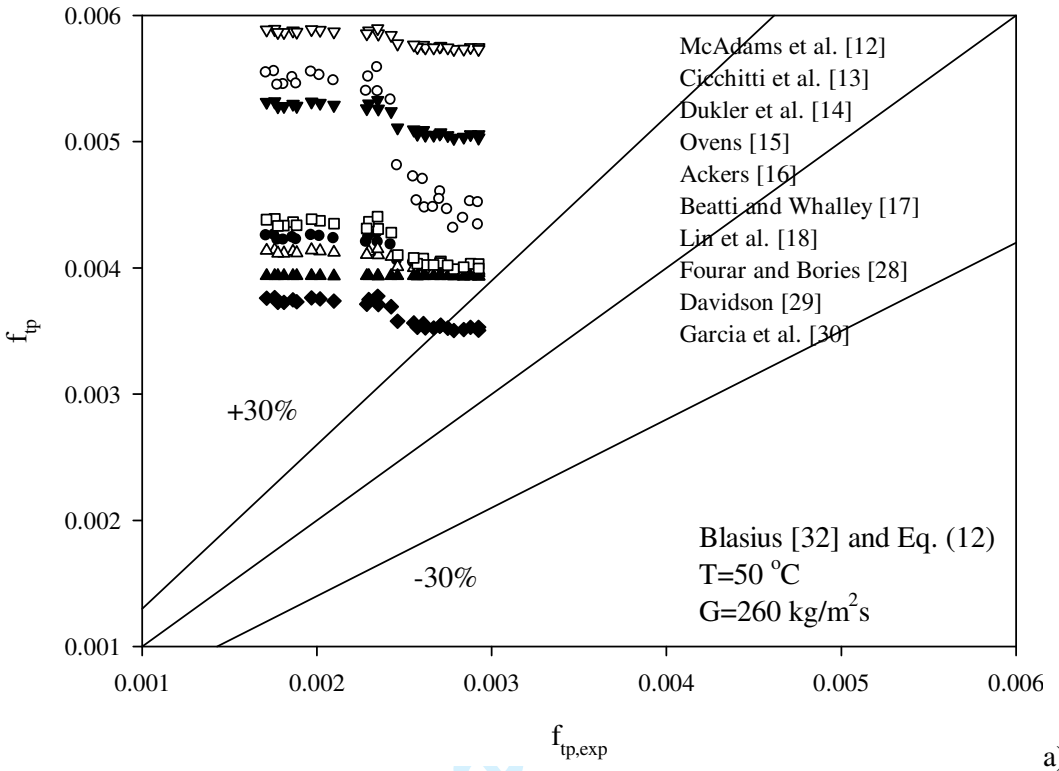


a)

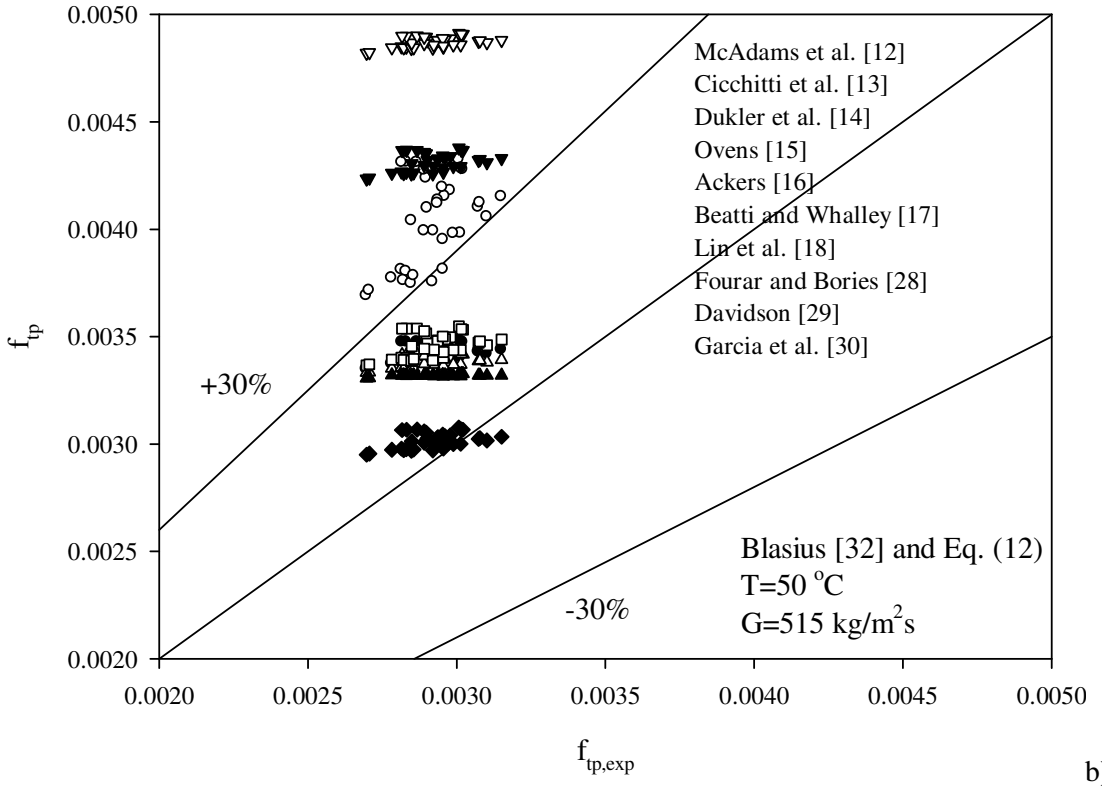


b)

Fig. 1 Comparison of two-phase friction factors obtained from Blasius [32] equation and Eq. (11)



a)



b)

Fig. 2 Comparison of two-phase friction factors obtained from Blasius [32] equation and Eq. (12)

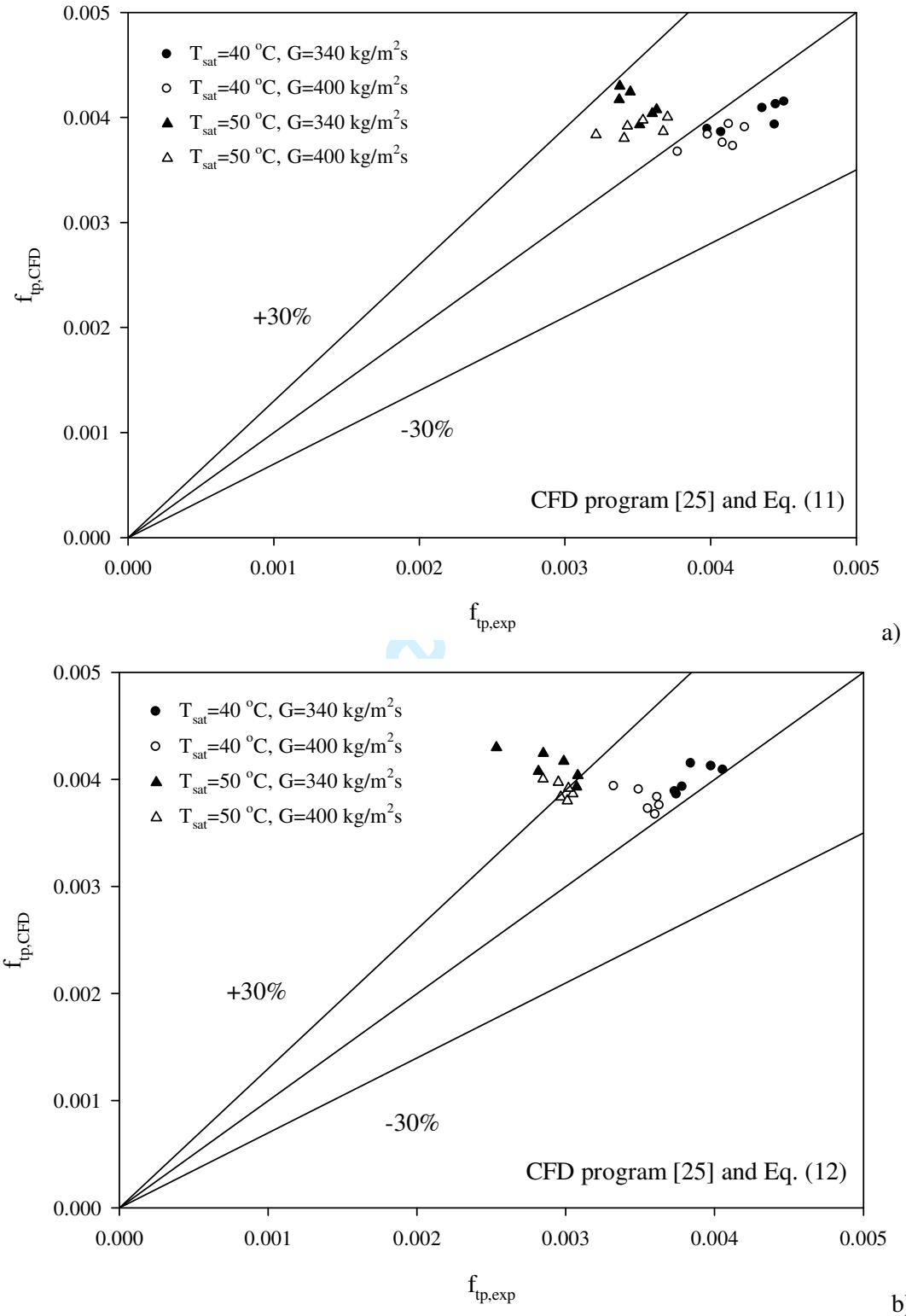
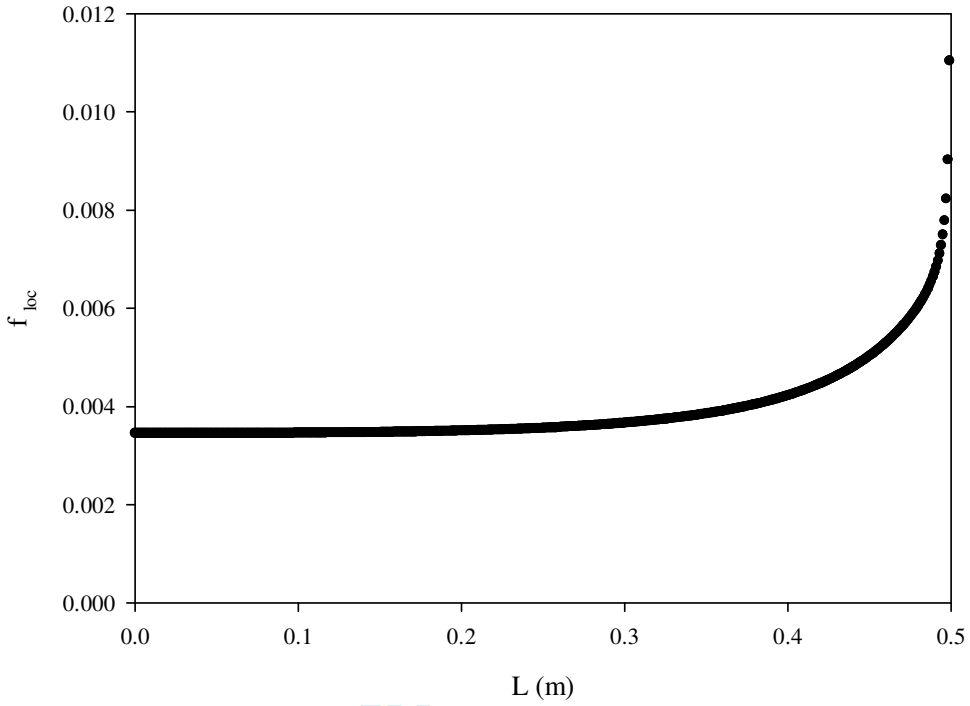
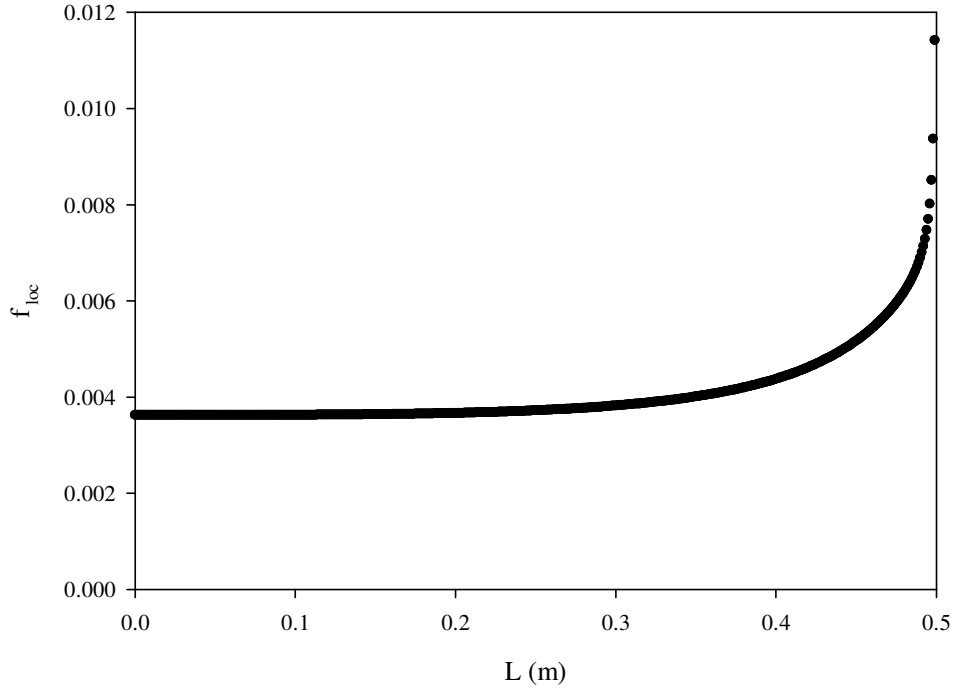


Fig. 3 Comparison of two-phase friction factors obtained from Eq. (11) (a) and (b) Eq. (12) and CFD program [25]

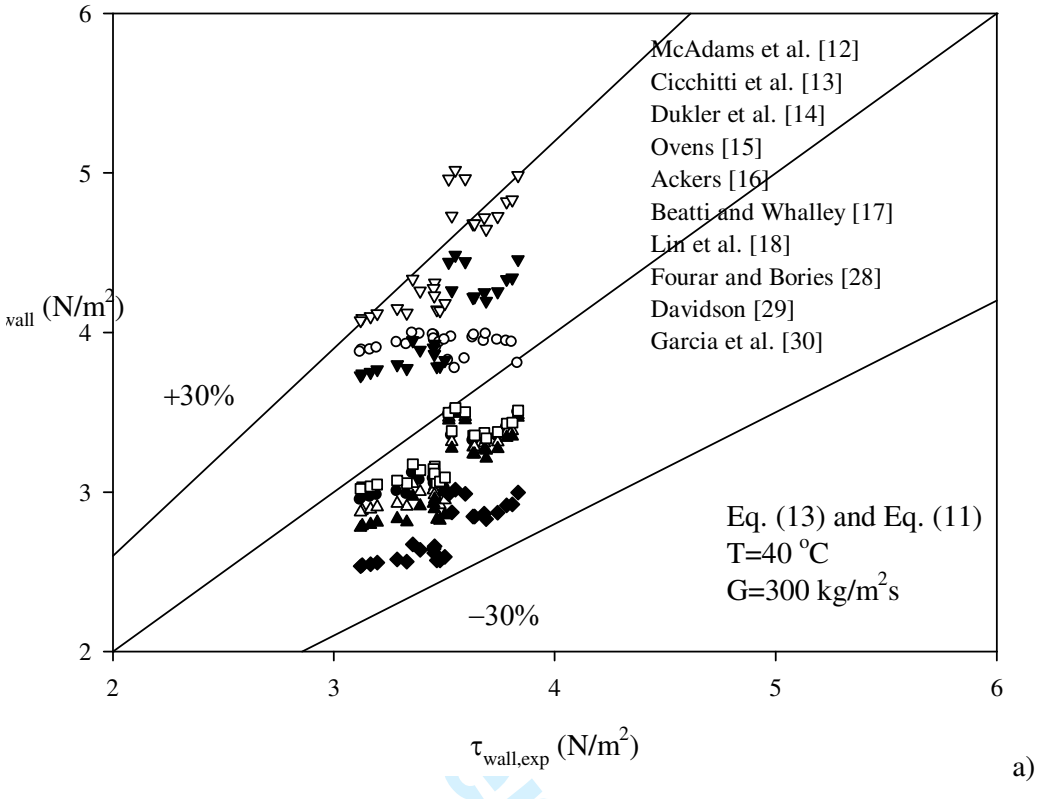


a) G=340 kg/m^{2}s, T_{sat}=50 ^{o}C, x=0.95



b) G=340 kg/m^{2}s, T_{sat}=50 ^{o}C, x=0.8

Fig. 4 Local alterations of two-phase friction factors obtained from CFD program [25] for various experimental conditions



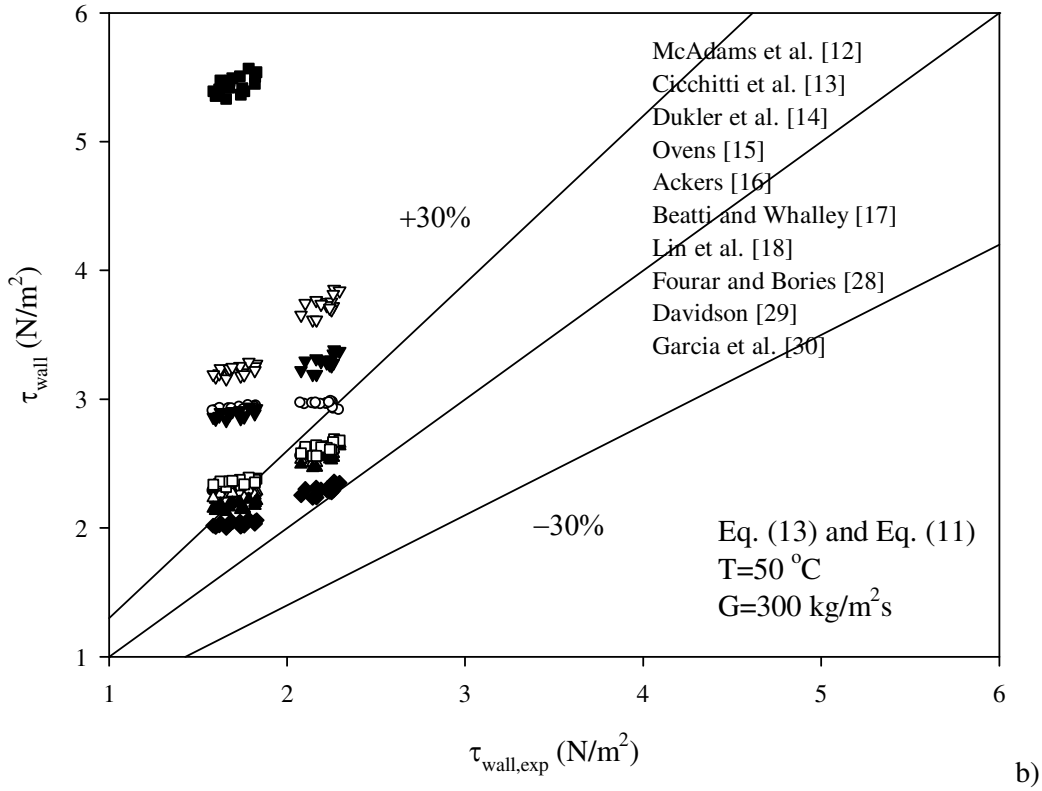
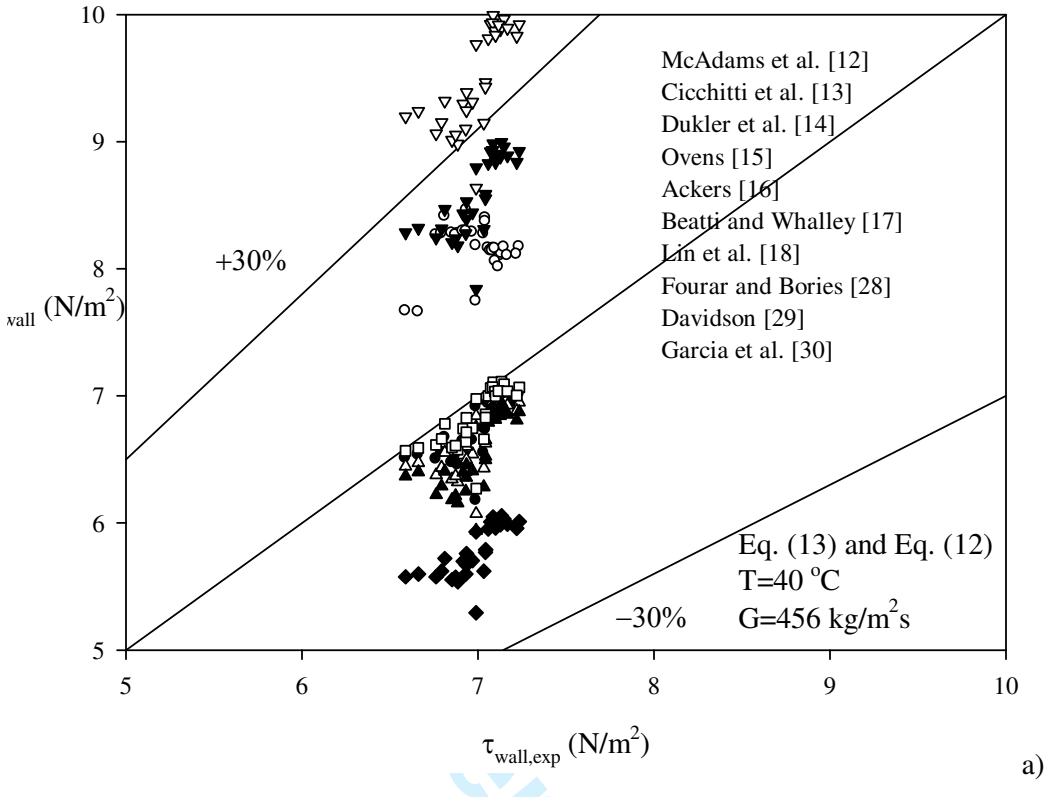
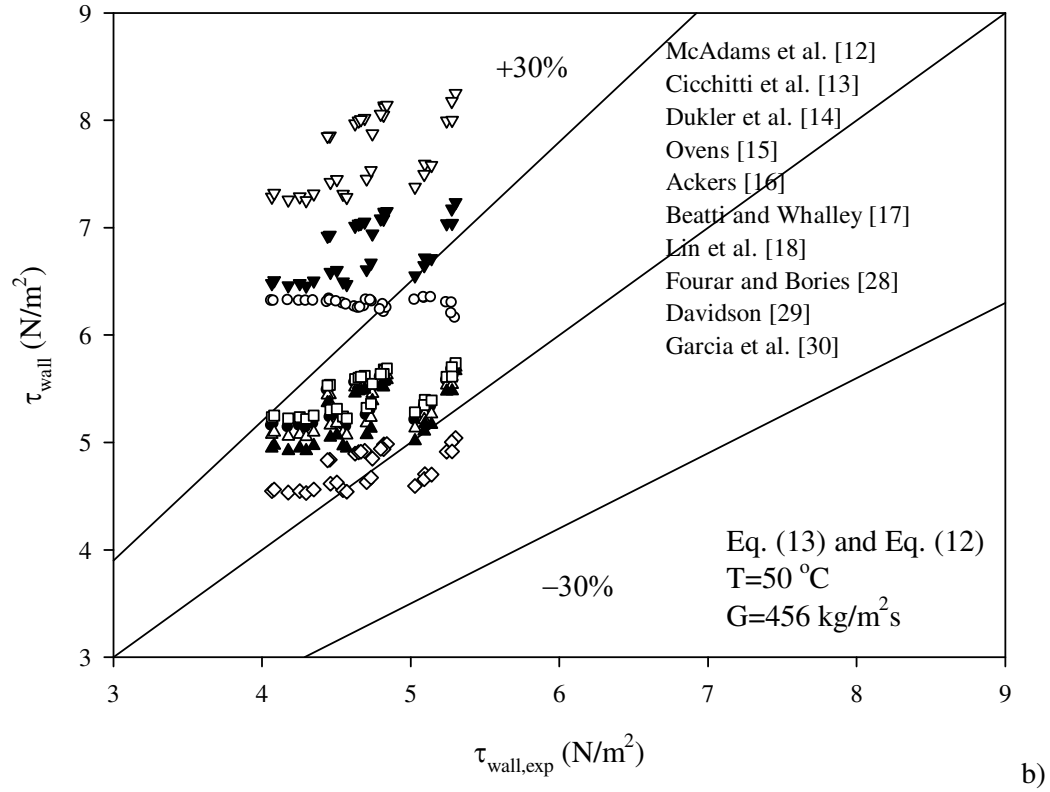


Fig. 5 Comparison of wall shear stresses obtained from Eq. (13) and Eq. (11)



a)



b)

Fig. 6 Comparison of wall shear stresses obtained from Eq. (13) and Eq. (12)

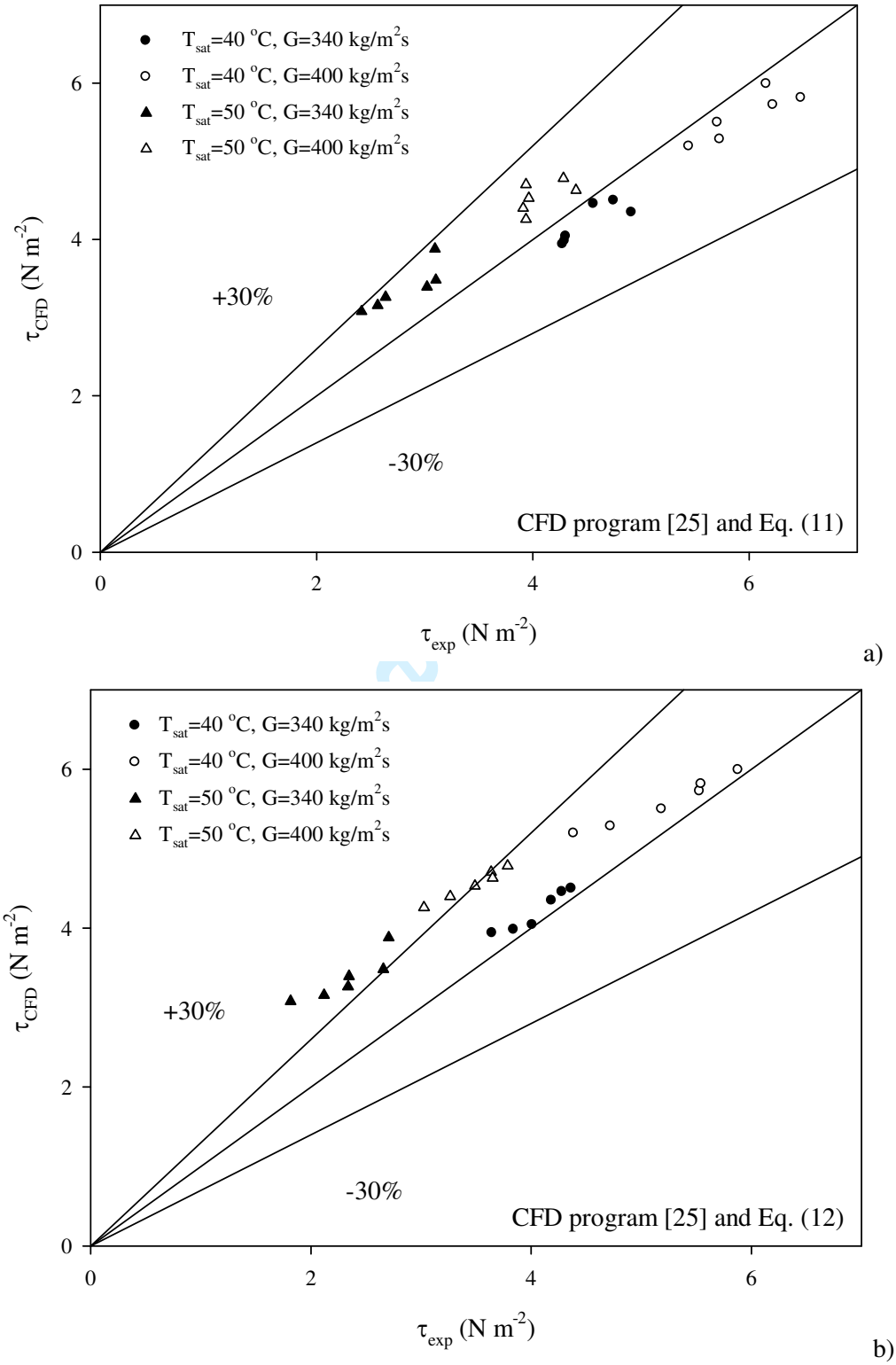
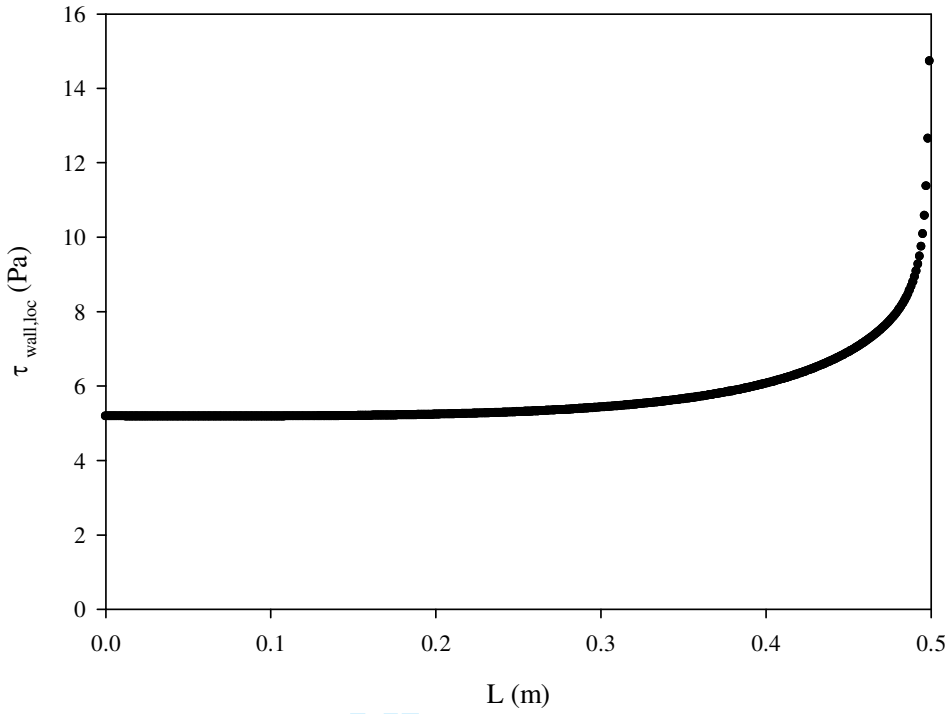
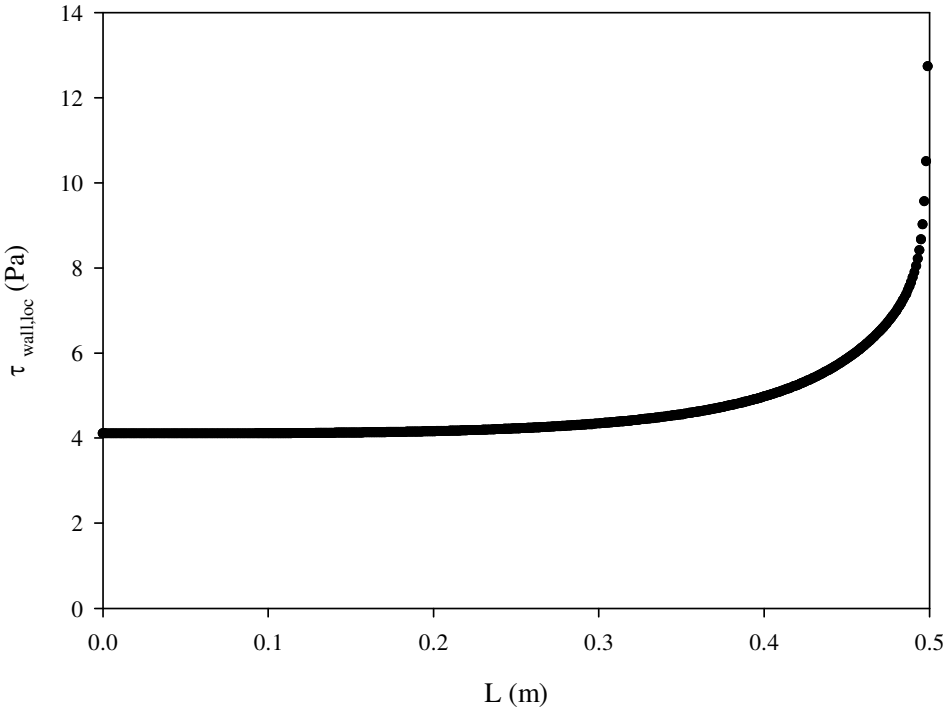


Fig. 7 Comparison of wall shear stresses obtained from Eq. (11) (a) and (b) Eq. (12) and CFD program [25]

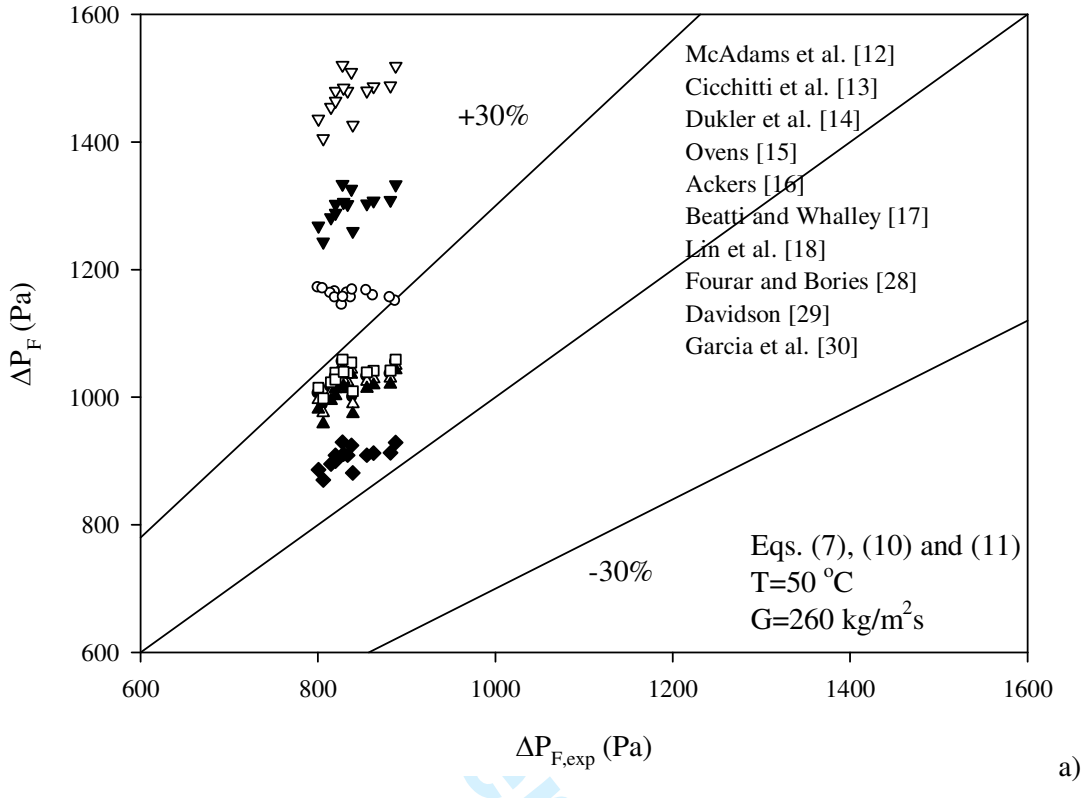


a)G=400 kg/m^{2}s, T_{sat}=40 ^{o}C, x=0.9

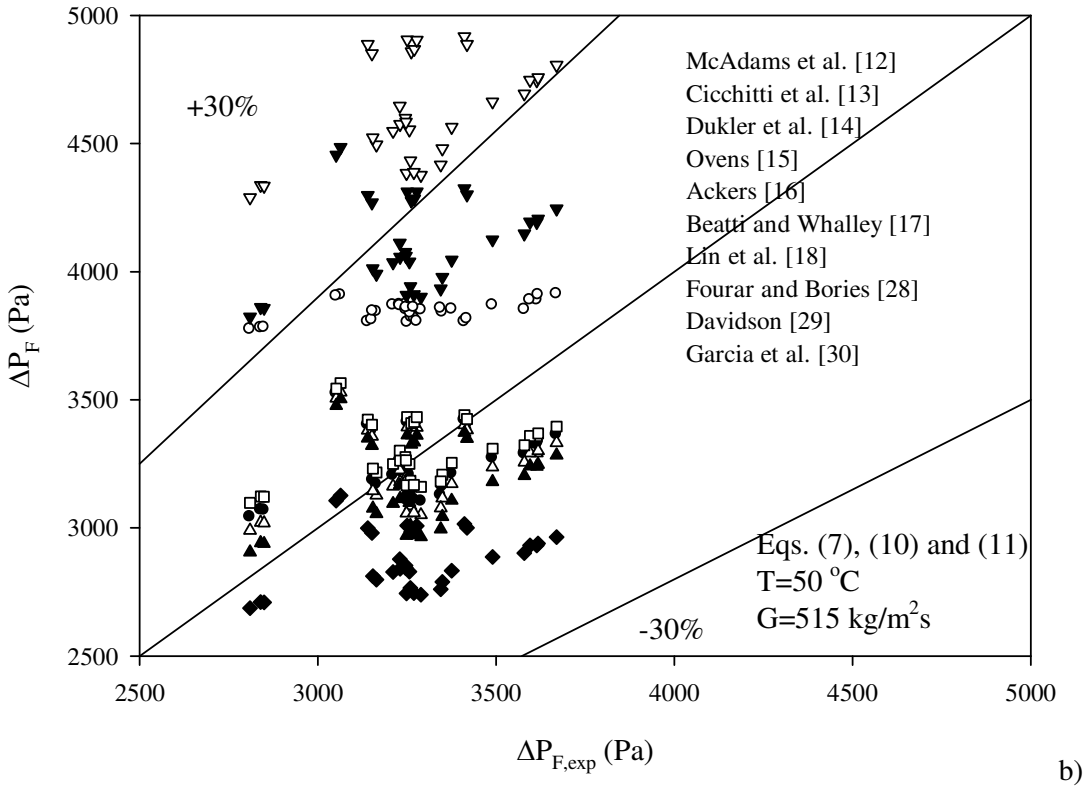


b) G=400 kg/m^{2}s, T_{sat}=50 ^{o}C, x=0.9

Fig. 8 Local alterations of wall shear stresses obtained from CFD program [25] for various experimental conditions



a)



b)

Fig. 9 Comparison of frictional pressure drops obtained from Eqs. (7), (10) and Eq. (11)

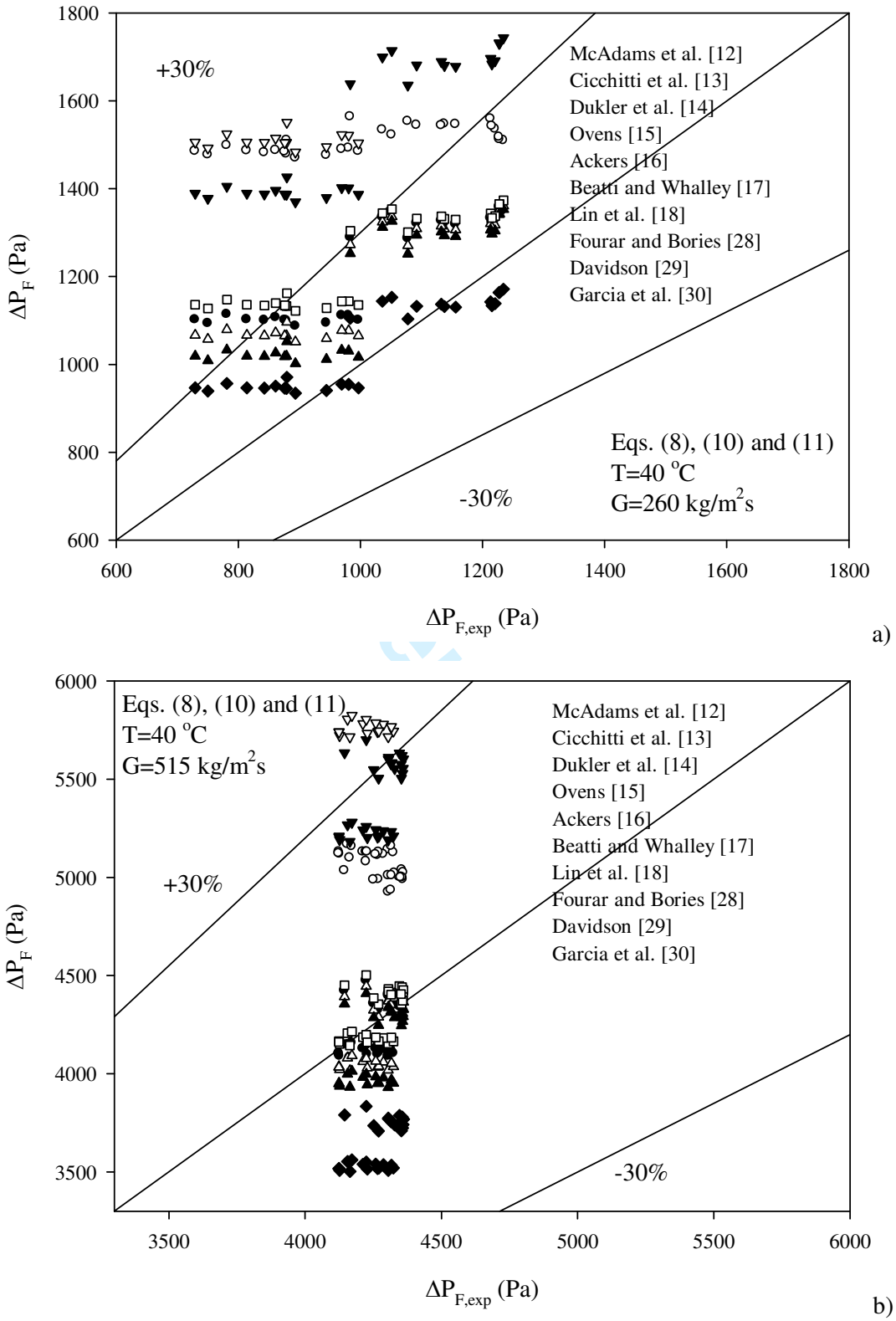


Fig. 10 Comparison of frictional pressure drops obtained from Eqs. (8), (10) and Eq. (11)

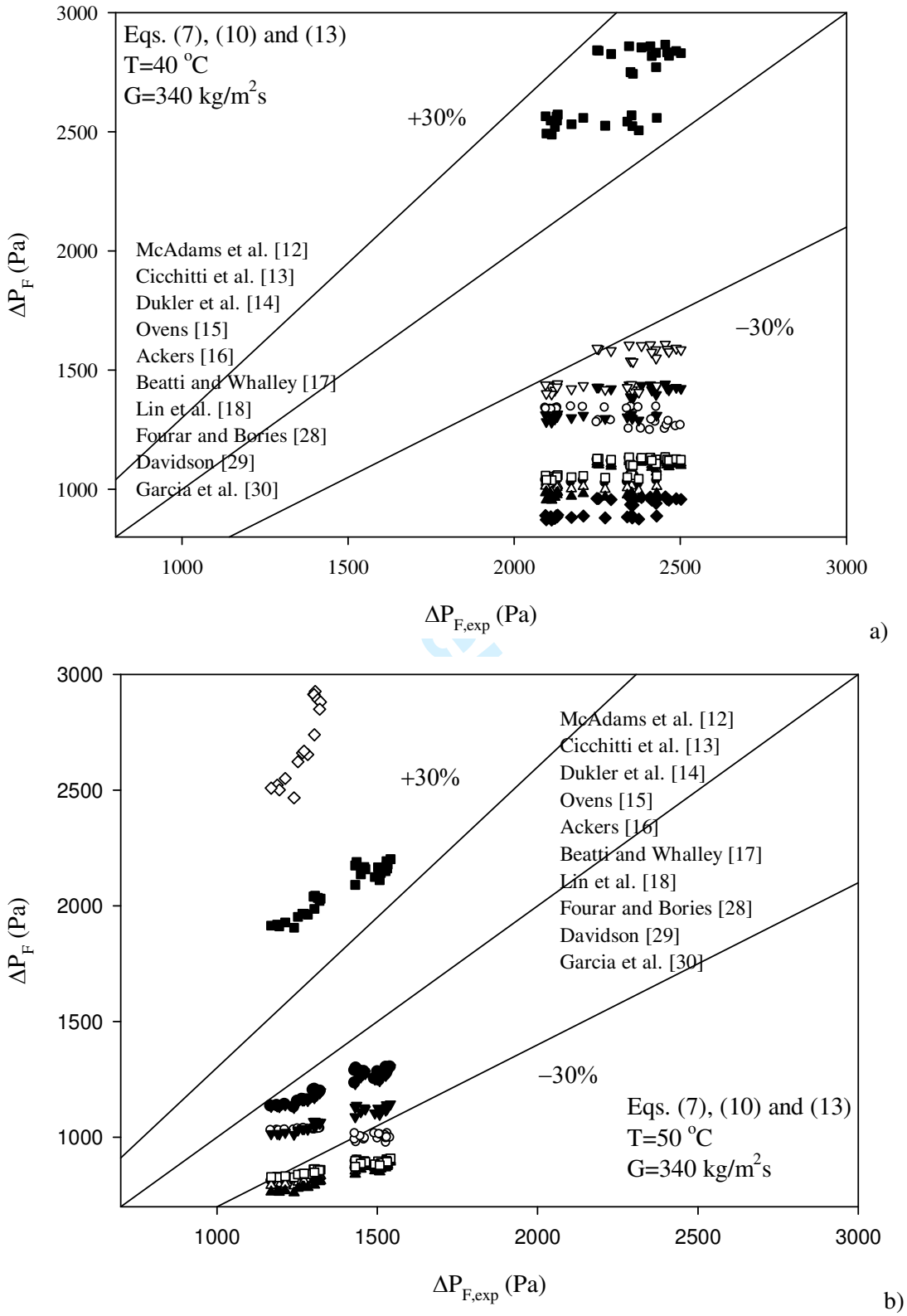


Fig. 11 Comparison of frictional pressure drops obtained from Eqs. (7), (10) and Eq. (13)

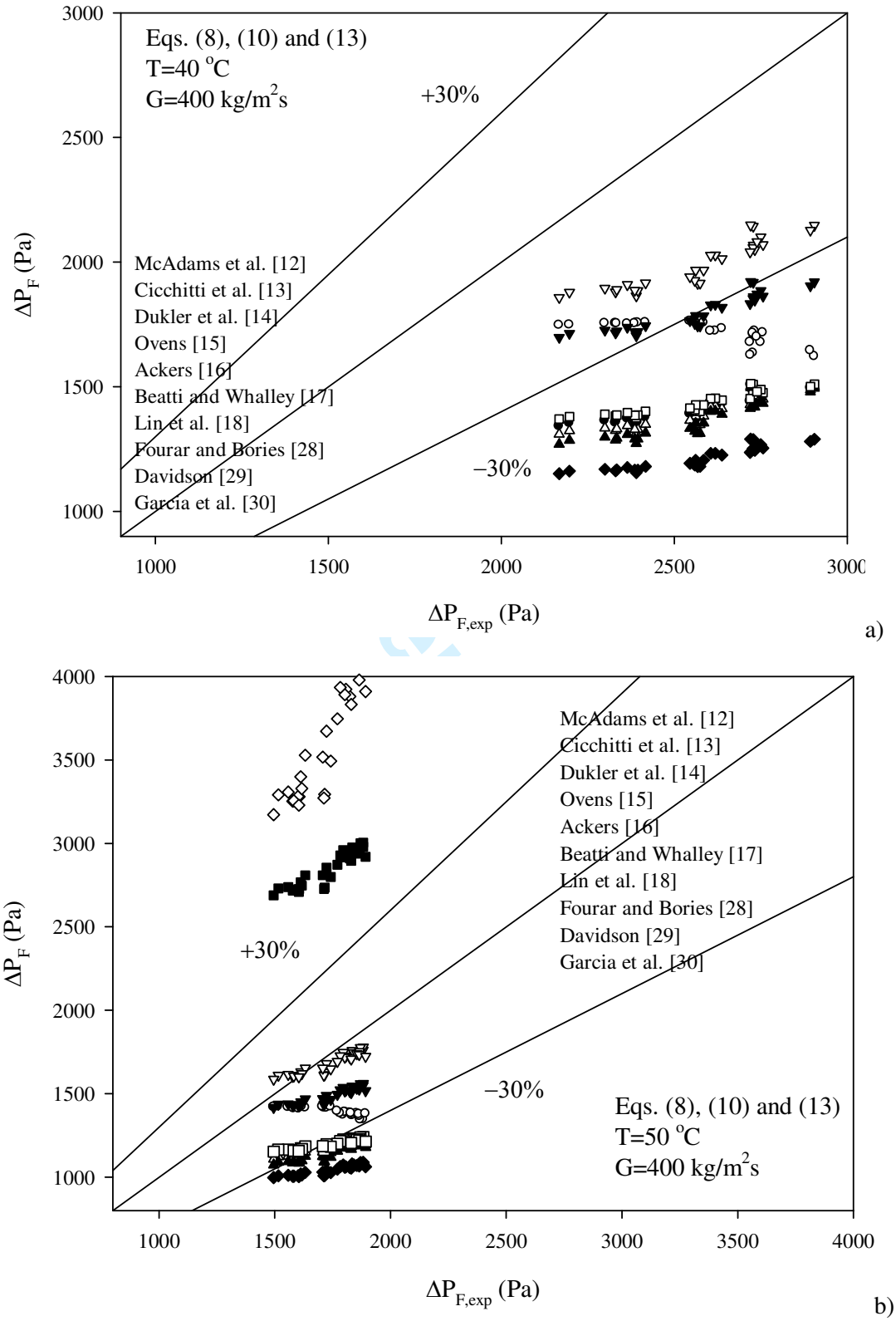


Fig. 12 Comparison of frictional pressure drops obtained from Eqs. (8), (10) and Eq. (13)

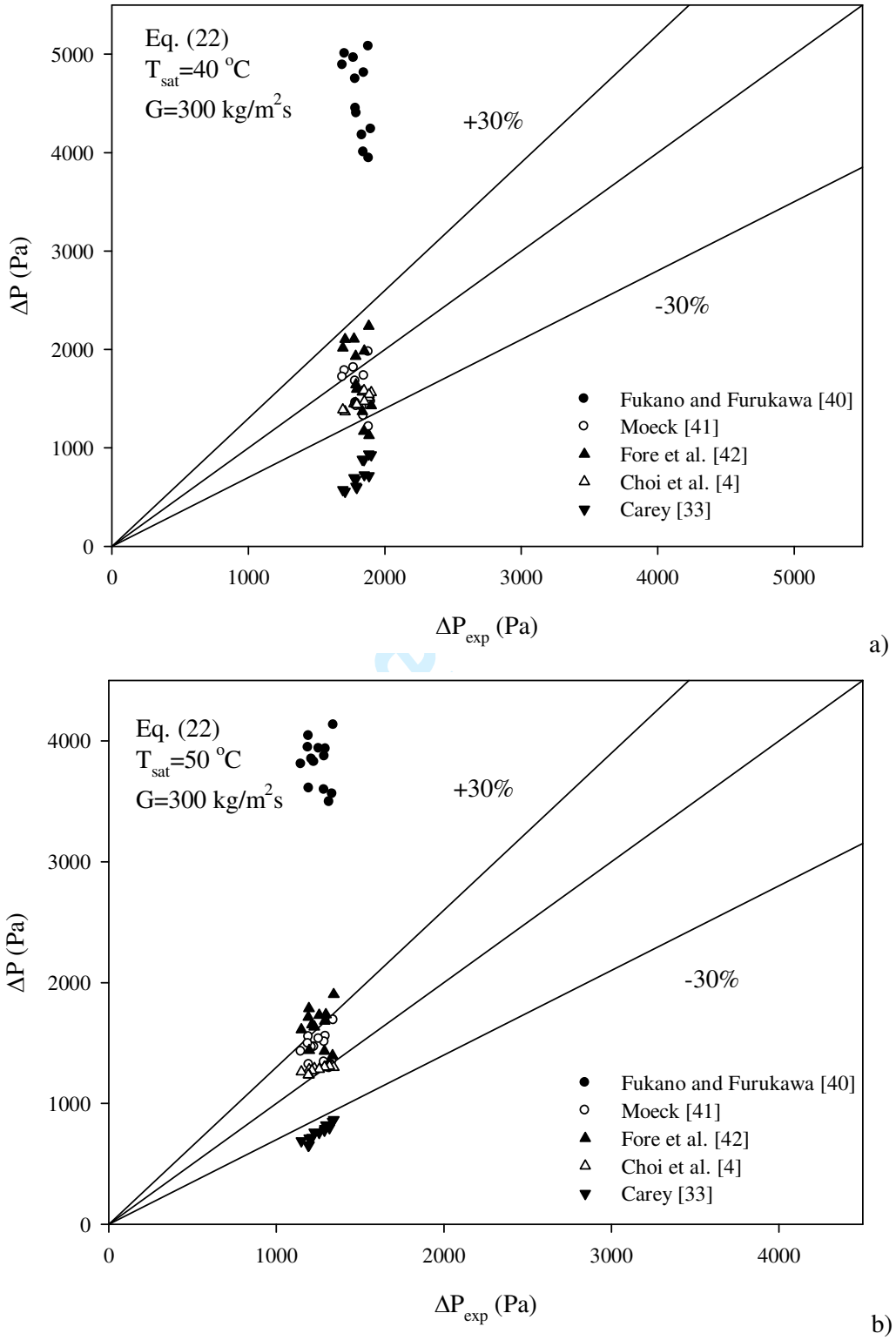


Fig. 13 Comparison of total pressure drop values between measured and calculated ones obtained from Eq. (22) during laminar flow of R134a

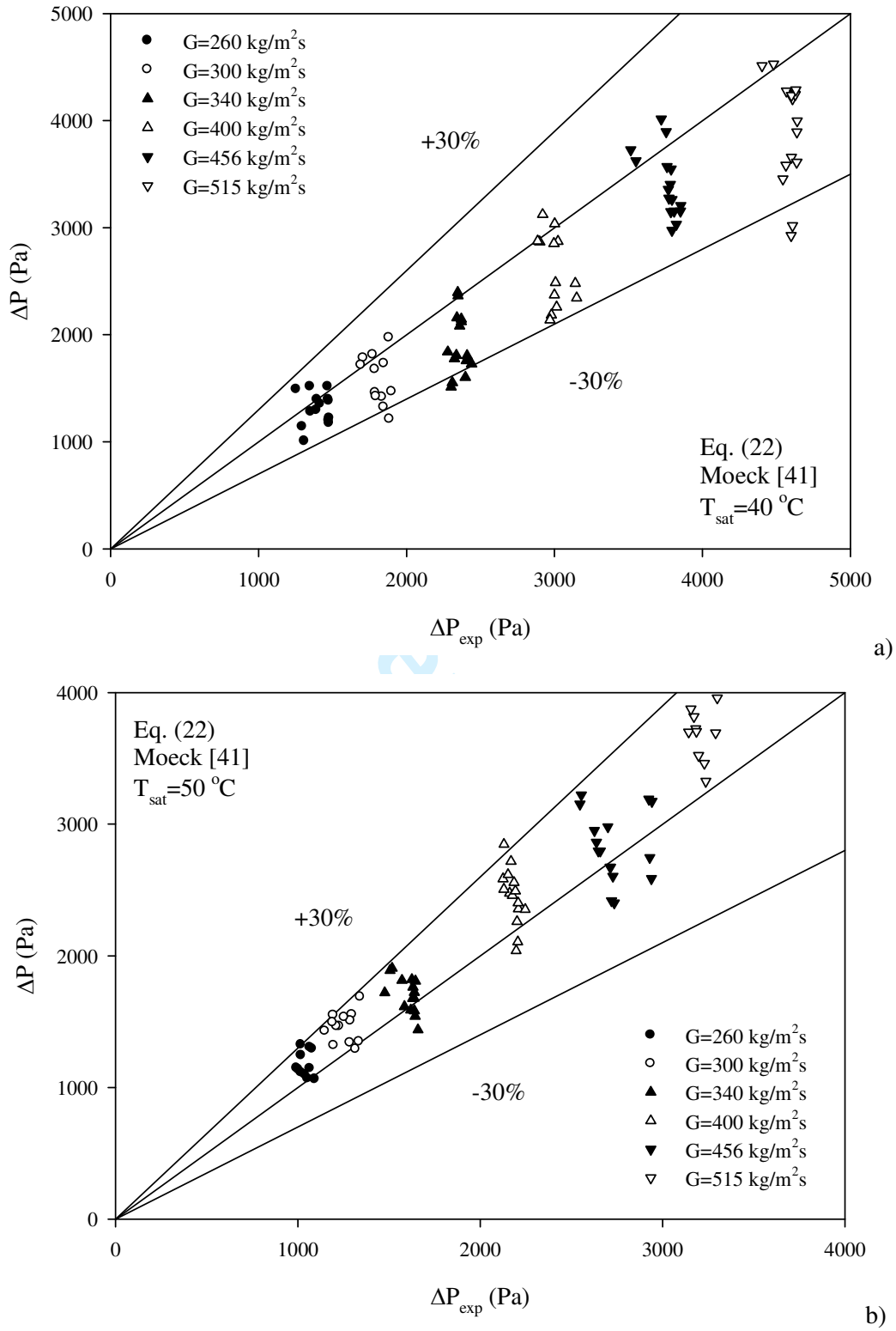


Fig. 14 Comparison of total pressure drop values between measured and calculated ones obtained from Eq. (22) and Moeck [41]'s two-phase friction factor during laminar flow of R134a

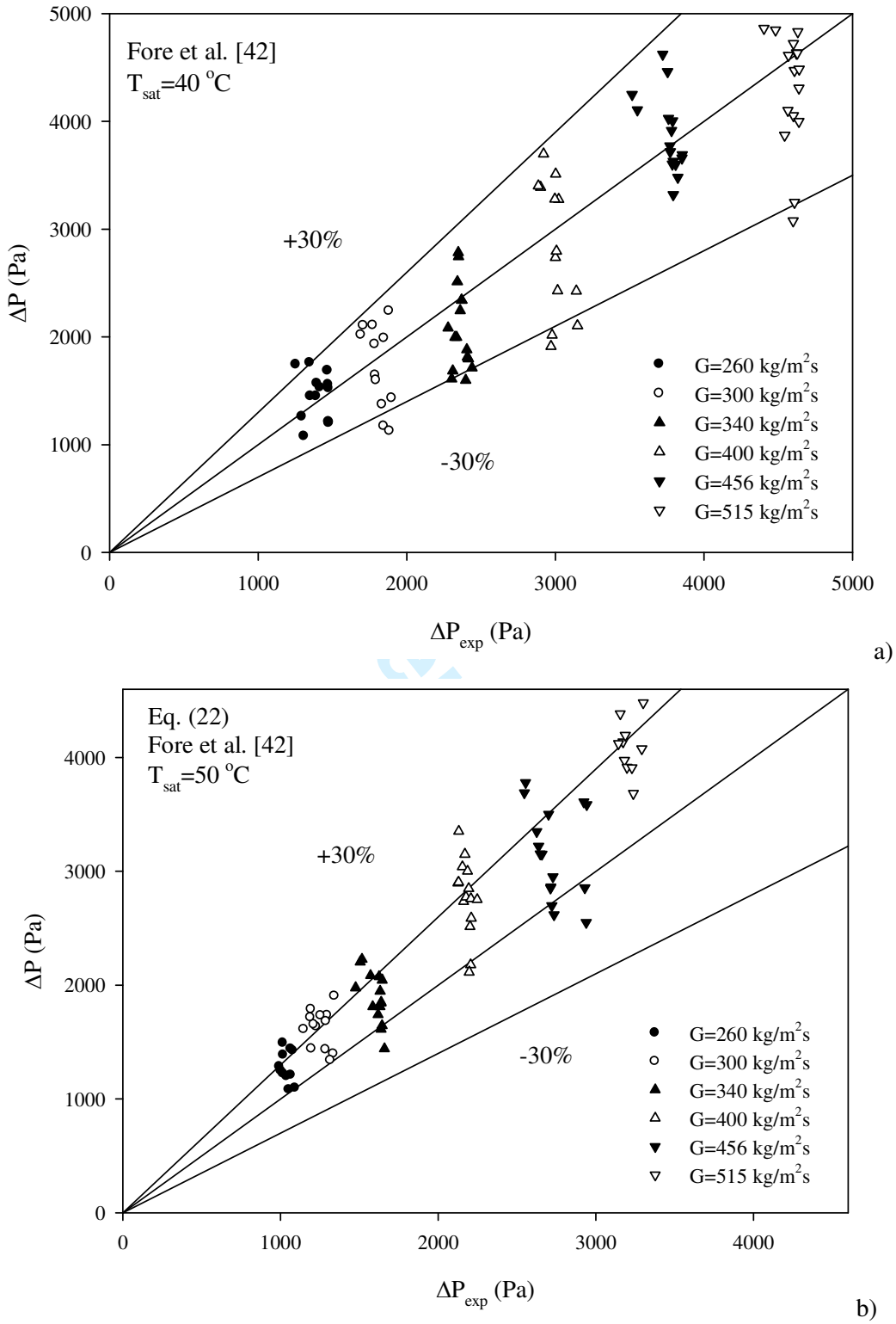


Fig. 15 Comparison of total pressure drop values between measured and calculated ones obtained from Eq. (22) and Fore et al. [42]'s two-phase friction factor during laminar flow of R134a

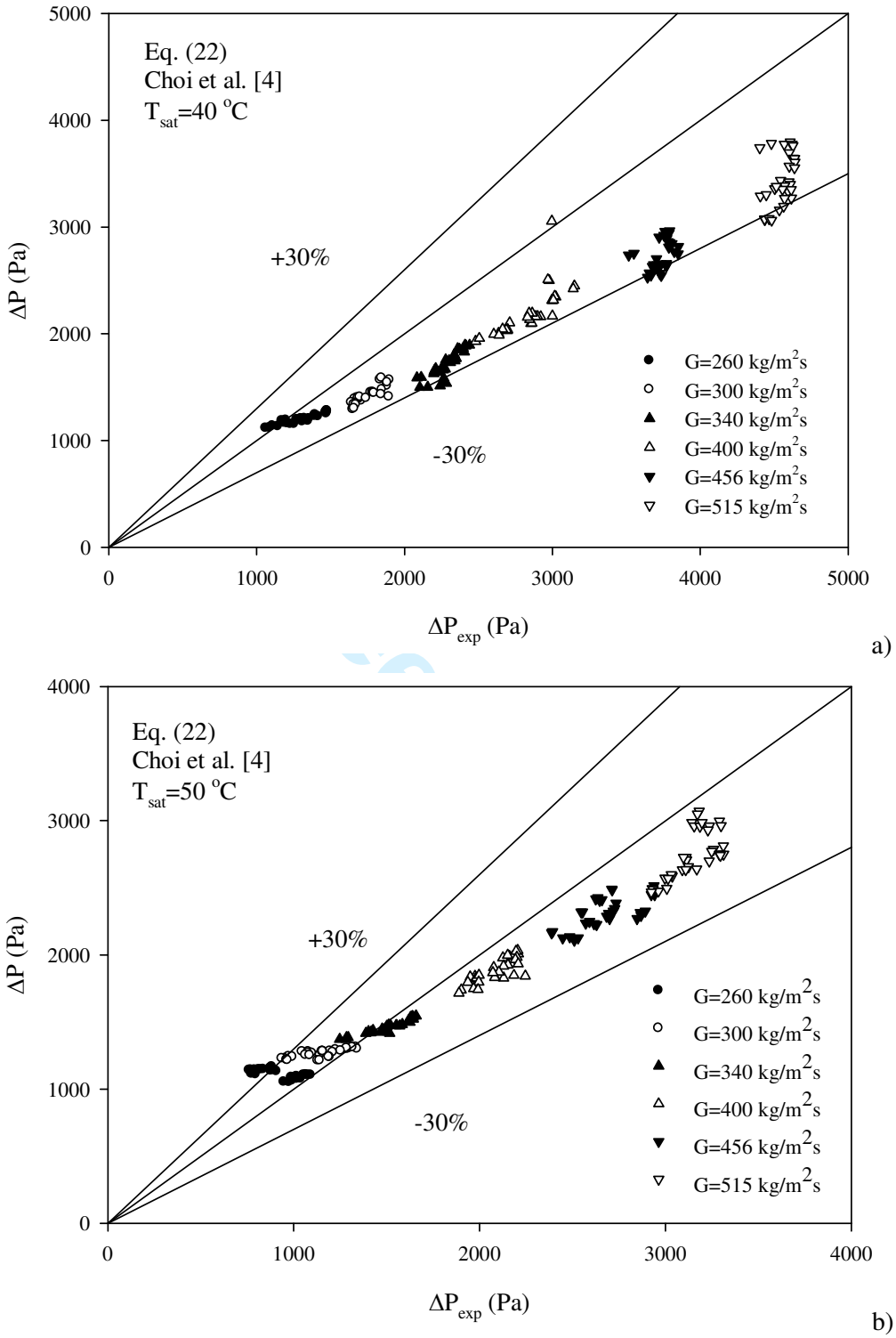


Fig. 16 Comparison of total pressure drop values between measured and calculated ones obtained from Eq. (22) and Choi et al. [6]'s two-phase friction factor during laminar and turbulent flows of R134a